Fault and fracture reactivation in the Penola Trough, Otway Basin

Thesis submitted in accordance with the requirements of the University of Adelaide for an Honours Degree in Geology

Bradley Thomas Grosser

November 2012

THE UNIVERSITY of ADELAIDE

FAULT REACTIVATION IN THE PENOLA TROUGH

ABSTRACT

The Penola Trough, onshore Otway Basin, is a failed rift structure trending NW-SE on the South Australian-Victorian border. Following its formation during the Late Jurassic, the trough has been subjected to alternating periods of extension and compression, leading to the reactivation under compression of many normal faults associated with the trough's formation during the rifting of Australia and Antarctica. Deposition of carbonaceous shales, fluviatile and lacustrine clastics and coals formed a hydrocarbon system, which has accounted for several successful plays to date. Several palaeo-hydrocarbon columns have also been drilled, with the absence of any oil or gas attributed to the reactivation of normal faults breaking the sealing mechanism present and allowing trapped hydrocarbons to migrate elsewhere. This project aimed to locate the fault segments that were most likely to dilate, slip and fracture and consequently the areas where hydrocarbons were unlikely to remain trapped. In contrast to this, geothermal exploration is targeted on the fault segments where reactivation is prone. Seismic interpretation and subsequent fault modelling was undertaken, and stress profiles containing stress and lithology data were applied to the interpreted faults, revealing reactivation likelihoods. Fault segments striking NW-SE at shallow depths (<2000m deep) were found to be the most prone to dilation. Shallow fault segments were also found most likely to fracture and slip. This correlates with current data showing known economic gas accumulations to be dominant on E-W trending fault traps. Carbon dioxide sequestration efforts would also be most successful on these sealing traps, while geothermal energy plays should target NW-SE striking faults and their associated fracture networks for optimal permeability.

KEYWORDS

Otway Basin, in-situ stress, fault reactivation, Penola Trough, fault, seismic

FAULT REACTIVATION IN THE PENOLA TROUGH

TABLE OF CONTENTS

FAULT REACTIVATION IN THE PENOLA TROUGH

LIST OF FIGURES AND TABLES

FAULT REACTIVATION IN THE PENOLA TROUGH

FAULT REACTIVATION IN THE PENOLA TROUGH

INTRODUCTION

The faults in the Otway Basin, derived from the continental rifting of Australia and Antarctica, are currently under the influence of compressional normal forces causing fault reactivation, as has been the case for much of the Cenozoic (Perincek & Cockshell 1995). Cementation of faults and poor-permeability phyllosilicates affect the faults, acting as sealing features (Boult *et al.* 2008). Movement of these faults can break the fault seal and produce damage zones, allowing fluid transmission and significantly impacting hydrocarbon, geothermal, carbon dioxide (CO_2) sequestration and other industries (Barbier 2002, Boult *et al.* 2008, Vidal-Gilbert *et al.* 2010).

Mapping the likelihood of reactivation of these faults can determine sections that may be preferentially aligned for reactivation with the in-situ NW-SE maximum horizontal stress, and hence transmit fluids. The present-day likelihood of fault reactivation and the history of fault reactivation in the basin are crucial for future hydrocarbon and geothermal exploration and production, as well as CO_2 sequestration exploration and production in the Penola Trough. Indeed, it is crucial in the remaining parts of the Otway Basin and many other sedimentary basins around the world.

The Penola Trough is a failed rift structure located towards the northern extent of the Otway Basin, straddling the South Australian-Victorian border (Figure 1). It trends NW–SE and is approximately 120km long by 40km wide. The trough is truncated on the southern edge by the northeast-dipping Hungerford-Kalangadoo fault system and shallows gradually toward the NE (Boult & Hibburt 2002) (Figure 1)

FAULT REACTIVATION IN THE PENOLA TROUGH

Figure 1. Outline of the western portion of the Otway Basin, showing the location and trend of the main structural features. The Balnaves/Haselgrove 3D seismic survey used for the study is included as an enlargement, along with wells within and in close proximity to the survey. Wells marked with a red circle indicate their use in the depth conversion and formation interpretation processes in Badleys TrapTester. The study area is outlined by the dashed red polygon within the inset map. (ST. C = St. Claire, BPT = Beachport)

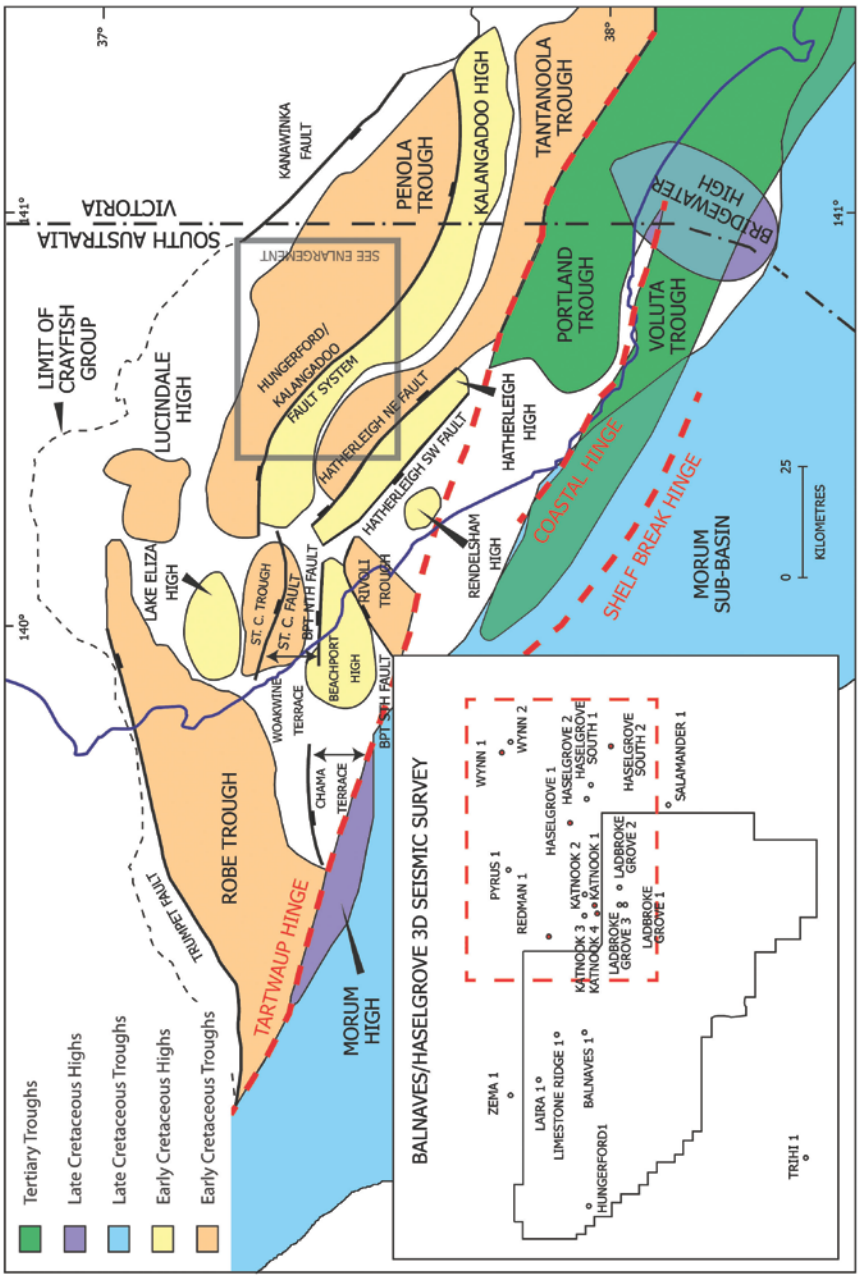

FAULT REACTIVATION IN THE PENOLA TROUGH

The rifting of Australia and Antarctica, which began during the Late Jurassic, created the Otway Basin, where carbonaceous shales, fluviatile and lacustrine clastics and coals were deposited from the Late Jurassic to the Miocene (Lovibond *et al.* 1995). Several marked unconformities are evident throughout the Otway Basin indicating compressional uplift events (Jensen-Schmidt *et al.* 2001) (Figure 2). Late Cretaceous seafloor spreading provided accommodation space for syn-rift sediments in the resulting NW–SE trending structures (Veevers 1986) (Figure 1), while post-Palaeogene compression changed the stress regime of the basin, causing normal faults to reactivate and form roll-over anticlinal structures, which are especially prevalent in the offshore Otway Basin (Cockshell *et al.* 1995).

The current compressional stress, sourced from the net torques of all related plate-boundary forces (Reynolds *et al.* 2002), has the ability to cause reactivation or formation of new faults (Lisle & Srivastava 2004). The likelihood of reactivation is able to be assessed by determining the in-situ stress field components, mechanical properties of the fault rock and existing fault geometry (Dewhurst *et al.* 2002). Faults in the Otway Basin generally trend E-W and NW–SE (Holford *et al.* 2011) and are influenced by a maximum horizontal stress oriented at approximately N128°E (Lyon *et al.* 2005b).

In this paper we test the hypothesis that faults striking NW – SE in the Penola Trough, Otway Basin, will allow fluid flow during the in-situ stress regime. We also test the hypothesis that faults would be more or less prone to

FAULT REACTIVATION IN THE PENOLA TROUGH

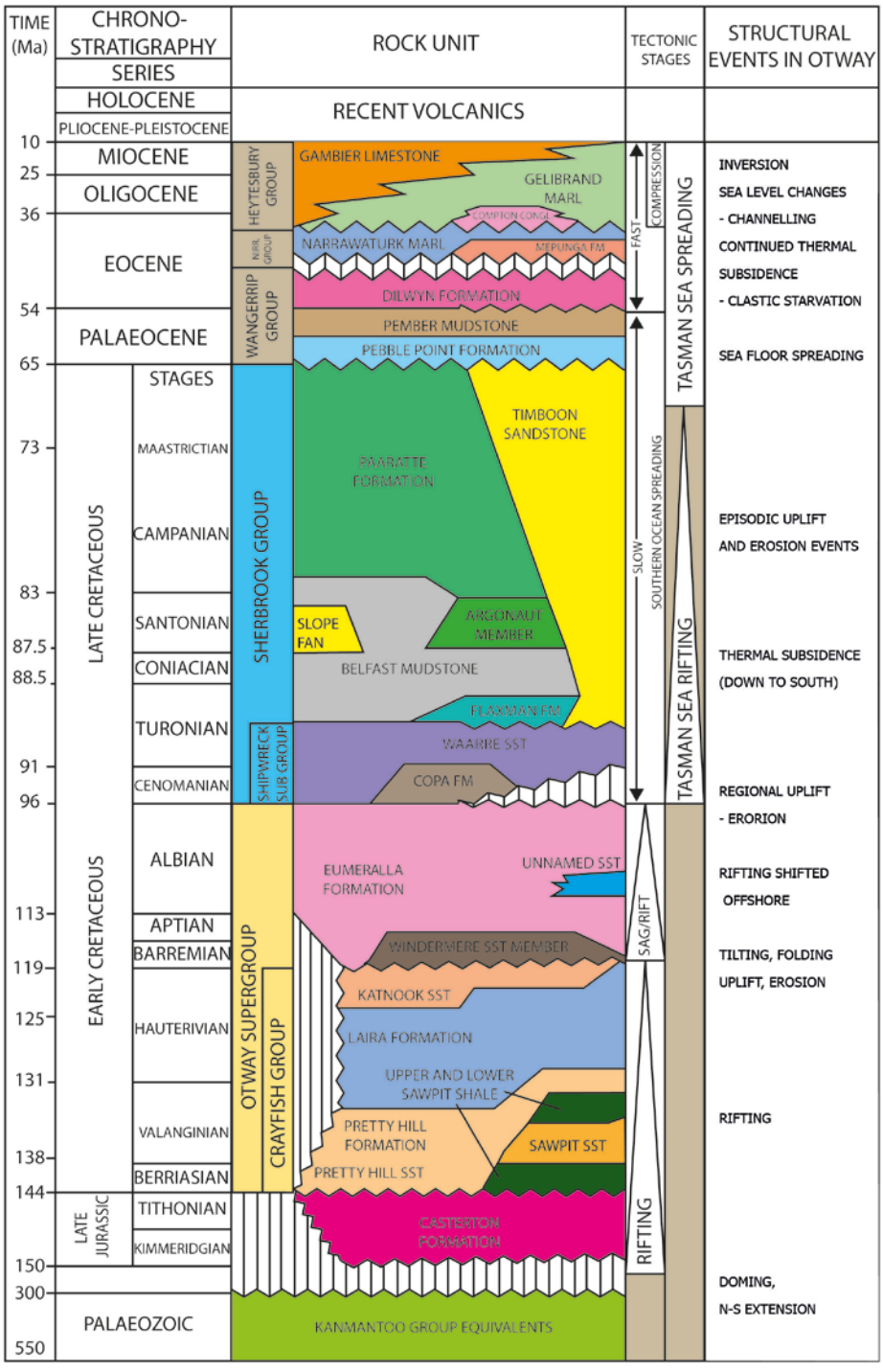

Figure 2. Chronostratigraphy and summary of tectonic events of the Penola Trough, Otway Basin (after Lyon *et al.* 2005, modified from Lovibond *et al.* 1993)

reactivation at different periods in the past, due to the differing palaeostress regimes. Movement of faults throughout history can give an insight into the evolution of the faults and associated sedimentary packages. Packages of syn-rift sediments and post-rift sediments demonstrate that faults in the Penola Trough have been both active and inactive throughout geological time.

In this study we interpret the reprocessed Balnaves/Haselgrove 3D seismic survey (Figure 1, enlargement), focusing primarily on fault structure and orientation. Following this, an assessment of reactivation likelihood of these faults was undertaken by looking at basin history, fault rock composition, pore-fluid pressure, in-situ stress fields and fault architecture. By applying variations of these data based on quality, reliability and proximity to the survey, the aim was to determine data combinations that would induce a high likelihood of reactivation, and to determine where these are located, with implications for hydrocarbon, geothermal and CO_2 sequestration industries.

The study also used palaeostress regimes with arbitrary stress magnitudes to determine which fault segments may have been likely to reactivate in the past. By using data from 55 million years ago (Ma), 23-11Ma and 11-6Ma (Muller *et al.* 2012), a pseudo-timeline of the Penola Trough's stress history was created. Palaeostress modelling data was coupled with migration timings, depths and maturities of hydrocarbons within the Penola Trough, which had the potential to yield information on the presence or absence

of a successful hydrocarbon accumulation, assuming the palaeostress models successfully showed periods when the fault was not sealing.

GEOLOGICAL SETTING/BACKGROUND

Geological History

LATE JURASSIC GRABEN FORMATION

The Otway Basin was formed as one of a number of basins during the breakup of Australia and Antarctica and the formation of the southern Australian margin (Norvick & Smith 2001). Rifting of the southern Australian margin began to the south of the Bight Basin during the Callovian, propagating eastwards towards the Otway and Gippsland basins by the Tithonian (Figure 2) (Norvick & Smith 2001). A series of half-grabens (Figure 1), which include the Penola Trough, were formed during this initial stage of extension (Perincek & Cockshell 1995).

LATE JURASSIC - EARLY CRETACEOUS RIFTING, BARREMIAN UPLIFT

During the Tithonian N-S extensional phase, E-W striking faults were formed (Teasdale *et al.* 2002). Initial sedimentation in the Penola Trough began with the lacustrine-dominated carbonaceous shale of the Casterton Formation (Boult *et al.* 2008) (Figure 2).

Escalated rifting in the Berriasian resulted in extensional reactivation of faults, allowing for the deposition of fluviatile and lacustrine clastics and coals of the Crayfish Group

which dominate the Penola Trough (Kopsen & Scholefield 1990, Lovibond *et al.* 1995) (Figure 2). The end to this extension is marked by tilting, folding and uplift of Crayfish Group sediments during the Barremian, leaving an angular unconformity in the Penola Trough (Jensen-Schmidt *et al.* 2001) (Figure 2).

Minor fault movement occurred during the deposition of the fluvio-lacustrine Eumeralla Formation during the Aptian-Albian (Figure 2), with evidence showing the depocentre moving to the south during the Albian (Palmowski *et al.* 2004), leaving the Penola Trough and other similar features as failed rift structures (Lovibond *et al.* 1995).

MID CRETACEOUS INVERSION

Regional uplift and erosion at the end of the Albian caused truncation at the top of the Eumeralla Formation (Figure 2) and separation of the Otway Basin from the Torquay sub-basin (Veevers 1986).

LATE CRETACEOUS EXTENSION AND SAG

Extrusion of oceanic crust began during the Cenomanian which coincided with the deposition of deltaic, marginal marine and deepwater Sherbrook Group sediments (Figure 2).

Following a period of thermal subsidence, the Otway Basin was subject to the final break-up of the continents in the Late Cretaceous, with slow seafloor spreading during the Maastrictian causing NE–SW extension (Krassay *et al.* 2004) (Figure 2). Rifting

was mainly focused offshore, having little effect on the Penola Trough (Boult *et al.* 2008). This extension not only formed new NW-SE oriented faults, but reactivated E-W striking faults formed during the Early Cretaceous (Lyon *et al.* 2004).

Aside from a eustatic low in the Maastrictian to Early Palaeocene resulting in formation of an unconformity at the top of Sherbrook Group sediments (Holdgate *et al.* 1986) (Figure 2), the Penola Trough was relatively quiet during the Mid to Late Cretaceous.

Sediments of the Otway Basin became gradually more marine-influenced from the Palaeocene to the present-day (Figure 2), with a progressively increasing calcareous nature indicating the establishment of open marine circulation (Blevin & Cathro 2008)

EARLY EOCENE INVERSION

The change from slow to fast rifting during the Eocene (Norvick & Smith 2001) caused compressional unconformities in the Early Eocene (Figure 2), which are found in many of the southern Australian margin basins (e.g. Gippsland Basin, Torquay Sub-Basin) (Holdgate *et al.* 2003, McGowran *et al.* 2004).

EOCENE-MIOCENE SAG

Continued thermal subsidence caused clastic starvation; resulting in minimal clastic input and allowing the deposition of marine carbonates of the Nirranda and Heytesbury groups, which dominate the stratigraphy (Lyon *et al.* 2005b) (Figure 2).

FAULT REACTIVATION IN THE PENOLA TROUGH

OLIGOCENE-RECENT INVERSION

The nature of the basin changed during the Oligocene, whereupon compressional deformation events began to dominate, due to changes in in-situ horizontal stresses from far-field plate boundary forces (Perincek & Cockshell 1995).

Collision of the northern and eastern Australian margins caused in-situ stresses to alter the nature of the basin from rapid NE-SW oriented seafloor spreading to a wrenching and compression scenario with a maximum horizontal stress oriented in a NW-SE direction (Perincek *et al.* 1994). Antiformal structures, trending NE-SW, and the inversion of existing faults were consequences of the changing stress field (Cockshell *et al.* 1995).

Late Miocene inversion structures and onshore Pliocene–Holocene features have parallel strikes, implying that both sets of structures were formed under a similar in-situ stress field (Sandiford 2002). Early Pliocene changes in coupling between the Indo-Australian and New Zealand plates have caused a strike-slip fault stress regime to affect the Penola Trough (Hillis *et al.* 1995). However, new leak-off testing methods have the capacity to yield alternate minimum horizontal stress magnitudes that would imply a reverse fault stress regime at present-day in the Otway Basin (King *et al.* 2012).

Geomechanical Background

Faults can have highly variable geomechanical properties (Dewhurst *et al.* 2002). These properties can affect the way a fault moves or holds under a given stress field.

FAULT REACTIVATION IN THE PENOLA TROUGH

Cementation type, shale levels, lithology juxtaposition arrangement, rock strengths and pore pressures all affect how a fault will respond when under stress. Along with these properties, the dip and strike of a fault and its relation to the in-situ stress-field can affect if or how it will reactivate.

CEMENTATION

Fluid sealing mechanisms can include cemented cataclasites, which form in deep sandstones; phyllosilicate framework fault rocks, which form in impure sandstones and clay smears; entrainment of shales into the fault zone (Fisher & Knipe 1998). Cemented faults are exceptionally strong, and can remain competent under higher shear stresses than intact surrounding rocks for the same effective normal stress. This causes virgin rock to fail before the fault itself. In such cases, fault orientation is irrelevant when discussing historical fluid flow through reactivation, as new fault formation is not constrained by the original orientation of the cemented faults (Dewhurst *et al.* 2002).

LITHOLOGIES AND JUXTAPOSITION

In the Penola Trough, the Laira Formation acts as a regional seal when juxtaposed with the Pretty Hill Sandstone reservoir (Dewhurst *et al.* 2002). Sand-on-sand juxtaposition seals are also present during some cases of faulting due to the presence of a shale gouge veneer (Lyon *et al.* 2005b). Reactivation of faults can render seals ineffective, allowing fluid to flow through faulted areas regardless of juxtaposition state or sealing caused by fault damage (Dewhurst *et al.* 2002).

FAULT REACTIVATION IN THE PENOLA TROUGH

Analysis of fractures in the Otway Basin by Jones *et al.* (2000) demonstrated that juxtaposition and fault deformation are both processes that are able to prevent fluid movement, explaining the existence of hydrocarbon palaeocolumns in the Otway Basin, such as that at the Zema-1 borehole (Figure 1). Jones *et al.* (2000) also state that Zema-1 required a sealing fault trap for hydrocarbon traces to be present. This sealing fault was inferred to have been preferentially oriented for reactivation, whereupon movement along this fault caused seal breach. Trapped hydrocarbons were allowed to migrate elsewhere, leaving the residual palaeocolumn. Open fractures within the cataclasite support this by providing a conduit for hydrocarbon migration away from the broken seal (Jones *et al.* 2000). The Zema-1 example may be indicative of any fault segments demonstrated by this study to be at high risk of reactivation.

PORE PRESSURES

The level of fracture stability for any given fault plane is determined by the increase in pore pressure (ΔPp) required to move a fault segment towards the failure envelope and hence cause reactivation (Dewhurst *et al.* 2002). A low ΔPp value corresponds to a fault likely to reactivate, whereas a high ΔPp signals a stable fault plane (Lyon *et al.* 2005b). Changes in pore pressures are pertinent to CO_2 sequestration techniques, which are being studied for use in the Otway Basin. By injecting CO_2 into reservoirs, pore pressure is increased and fault stability is consequently reduced in zones surrounding the CO_2 plume (Vidal-Gilbert *et al.* 2010). Unstable, and hence permeable, faults are undesirable as they allow vertical leakage of the CO_2 (Vidal-Gilbert *et al.* 2010).

FAULT REACTIVATION IN THE PENOLA TROUGH

STRESSES AND FAULTS

Andersonian faulting theory (Anderson 1951) dictates that the angles of principal stresses in relation to a fault plane will determine the faulting regime that will occur. A maximum principle stress (σ_1) that is vertical will cause normal faulting; horizontal and perpendicular to the fault strike will cause reverse faulting; while under a strike-slip stress regime faults will form at 26-30° to the maximum horizontal stress (σ_H) (Anderson 1951, Healy *et al.* 2006).

Existing faults will reactivate if the shear stress exceeds frictional resistance of the fault (Lisle & Srivastava 2004). When the ratio of shear stress to normal stress is high, the plane is unstable and slip is likely (Lisle & Srivastava 2004). Changes in applied load or fluid pressures can cause reactivation of fault planes by changing the effective stress applied to the rocks, moving the fault plane towards failure (Bell 1996). By experimentally testing faulted core rock, the Griffith-Coulomb Failure Criterion can be determined (Twiss & Moores 1992), and the conditions for failure defined where the angle of the failure plane intersects the failure envelope (Bell 1996).

STRESS ORIENTATIONS

According to Andersonian faulting theory, the three principle stresses can be resolved into a vertical stress (σ_v) and two horizontal stresses (a maximum, σ_H, and a minimum, σ_h) (Anderson 1951). The horizontal in-situ stress orientations can be inferred from Earthquake focal mechanisms, borehole failure, such as borehole breakouts and drilling-induced tensile fractures; as well as engineering-type measurements, such as leak-off-

tests (LOTs) (Bell 2003). Compressional in-situ stresses acting on the borehole can result in an ellipsoidal shaped borehole cross section, with elongation occurring perpendicular to the maximum horizontal in-situ stress, in the direction of minimum horizontal in-situ stress. Similarly, drilling induced tensile fractures (DITFs) can occur in the same orientation as the maximum horizontal stress due to tensile failure of the borehole wall (Aadnoy 1990) (Figure 3).

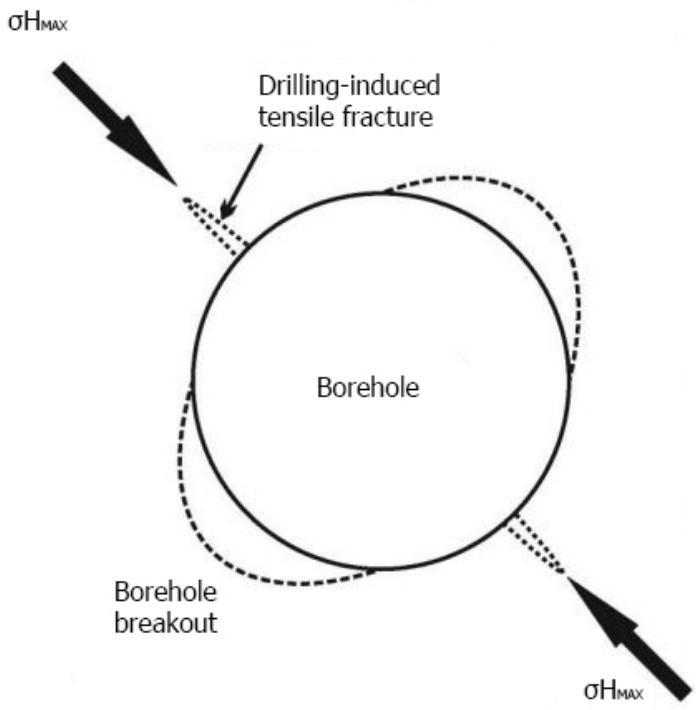

Figure 3: Cross-section of a borehole illustrating the position of borehole breakout and DITFs relative to in-situ horizontal maximum stress (σ_H) in a vertical wellbore (after Reynolds and Hillis (2000)).

After determining the orientation of either σ_H or σ_h, the other can be determined as they are oriented 90° from one another (Bell 2003). Anomalous variations in horizontal

stress direction can be attributed to local variations in geomechanical rock properties, such as fault zones and other subsurface factors (Bell 2003). Geomechanical rock properties influence the principal stress directions by causing the rotation of σ_H towards a hard or stiff interface so that it becomes perpendicular, but will rotate it to become parallel to a soft interface (Bell 1996, King *et al.* 2012).

In general, sedimentary cover directly overlying basement rock will reflect the stress orientations and magnitudes within the basement rock itself. However, a detachment layer, such as salt or hydrous shale, present immediately above the basement (and below overlying sediments), results in mechanical decoupling of the stress regime associated with the basement from the stress regime in the overlying sediments (Bell 1996). This may result in variable σ_H directions in the overlying sediments (Bell 1996, Tingay *et al.* 2011).

The in-situ stress field in the Otway Basin has a σ_H oriented towards N125°E in the western Otway Basin rotating to N139°E towards the Gippsland Basin in the east (Nelson *et al.* 2006). Lyon's (2005b) analysis of borehole breakouts in image logs gives the σ_H in the Penola Trough to be oriented towards N128°E, which is similar to the value of N125°E obtained by both Hillis *et al.* (1995) and Nelson *et al.* (2006). This is not parallel to the N to NNE absolute plate motion and is attributed to heterogeneous plate boundary forces on the northern and eastern plate margins (Hillis *et al.* 1998, Reynolds *et al.* 2002). Rotations in σ_H direction from E-W in Western Australia to N–S

in central and northern Australia are also reflective of the plate boundary forces (Hillis & Reynolds 2002, Reynolds *et al.* 2002).

In-situ stress measurements from sedimentary rocks generally record the present day's stress regime and will be uninfluenced by any palaeostress regimes (Bell 1996). Instead, modelling techniques (e.g. Muller *et al.* (2012)) have the capabilities to give palaeostress magnitudes and directions based on formulated plate boundary forces.

STRESS MAGNITUDES

Vertical stress magnitudes (σ_v) are equivalent to the weight of overburden at a specific depth. Therefore, magnitudes can be calculated from integration of log densities of the overlying sedimentary strata (Engelder 1993). The vertical stress gradient for the Penola Trough was determined to be 21MPa/km (Lyon *et al.* 2005b), which is slightly below the average value of 22.4 MPa/km (1 psi/ft) often assumed for sedimentary basins (Dickinson 1953, Tingay *et al.* 2003), but similar to work by Nelson *et al.* (2006) who calculated a value of 21.182MPa/km.

Horizontal magnitudes of stress can either be measured or estimated. The magnitudes can be measured by leak off and mini/micro fracture tests and estimated from failure simulations and equations involving tensile strength, pore pressure and fracture breakdown pressure (Bell 2003). In the Penola Trough, the σ_H gradient was determined to be 28.8MPa/km and σ_h gradient 15.5MPa/km (Lyon *et al.* 2005b). Values obtained

by Nelson *et al.* (2006) of 29MPa/km (σ_H) and 15.5MPa/km (σ_h) concur with Lyon's values.

FAULT ACTIVATION AND REACTIVATION

It has been suggested that lithospheric thickness (Tuitt *et al.* 2011) and thermal structure of the crust and lithosphere (Holford *et al.* 2011) can act as controls for reactivation and fault initiation. Thinner and warmer, weaker lithosphere appears to be preferential for reactivation (Holford *et al.* 2011, Tuitt *et al.* 2011), with the Otway and Gippsland basins having a relatively high heat flow compared to the other southern Australian margin basins (Holford *et al.* 2011).

The dip and orientation of faults is crucial to their reactivation likelihood. Faults located in the onshore Otway Basin generally dip NW, with smaller antithetic faults dipping SW (Boult 2001). Significant variations in reactivation risk along faults with the same strike azimuth can be attributed to changing dip angles (Dewhurst *et al.* 2002). Faults in the Penola Trough generally display consistent orientations and can be linked to basement faulting, causing similar faults to develop in the sedimentary deposits above (Dewhurst *et al.* 2002). In the Otway Basin, Early Cretaceous faults strike E-W, while Late Jurassic faults and shallower post-rift faulted sediments show fault orientations which reflect the changing stress profile and strike NW-SE (Lyon *et al.* 2004).

FAULT REACTIVATION IN THE PENOLA TROUGH

SEISMIC INTERPRETATION METHODS

The combined and reprocessed Balnaves-Haselgrove 3D seismic survey was loaded into SMT Kingdom Seismic Interpretation Package 8.6 for an initial seismic interpretation. Using wavelet amplitudes the location and shape of faults, horizons and selected sedimentary packages present within an area of the Penola Trough, onshore Otway Basin, were constrained. Interpretations were based on amplitudes viewed in two-way-time vertical seismic sections on arbitrary seismic lines, oriented to maximize the visibility of the faults. Horizons were identified by their high amplitude reflections (positive or negative), and were verified by comparing two-way-times with formation-top well control data from 33 wells within the survey or surrounding area (~15km around the survey). Faults were identified by their low amplitude reflections, especially evident when using a 200-colour gradient black-to-white colour display, as well as the displacement of horizons along fault planes. A complete method can be found in Appendix A.

SEISMIC INTERPRETATION DATA LIMITATIONS

Due to the limited resolution associated with seismic data, errors can be expected where high levels of resolution are needed to define small-scale structures (Kearey & Brooks 1991). Subseismic features such as fault-relay zones and fractures associated with damage zones around faults are often undetectable in seismic data (Kearey & Brooks 1991, Lyon *et al.* 2005b) and they are a key factor in assessing hydrocarbon prospect integrity and subsurface permeability for geothermal plays (e.g. Lyon *et al.* 2005b).

Thus, without a detailed understanding of the small-scale features associated with faulting, the interpretation's integrity cannot be guaranteed. However, comparison between the seismic interpretation and dipmeter data around borehole locations could reveal small-scale features in close proximity to the borehole, such as faults and fractures, which were previously undetectable (Backé *et al.* 2011, Abul Khair *et al.* 2012).

The vertical scale of the seismic data can become skewed at depth when being viewed in the time domain, affecting the magnitudes of throw on the faults in question. Depth conversion and tying seismic interpretation to borehole data can remove much of this uncertainty. However, uncertainty levels do rise with increasing distance from the borehole data, causing the depth conversion to be most accurate near well ties. Six wells were used for both the depth conversion process and for tying horizon interpretations. An additional 27 wells were located within or in close proximity to the survey, and incorporating the data from these wells in the depth conversion or horizon interpretation process would have increased the accuracy of both aspects.

STRUCTURAL GEOMETRIES FROM SEISMIC INTERPRETATION

Balnaves/Haselgrove 3D Seismic Interpretation

The initial structural interpretation of the reprocessed Balnaves/Haselgrove 3D seismic survey revealed the strike and dip of faults in the Penola Trough, Otway Basin, as well as the fault plane roughness and amount of vertical and horizontal displacement (throw

and heave). An initial interpretation revealed a series of grabens and half-grabens, dipping steeply towards either N to NNE or S to SSW (Figure 4b). These steep fault

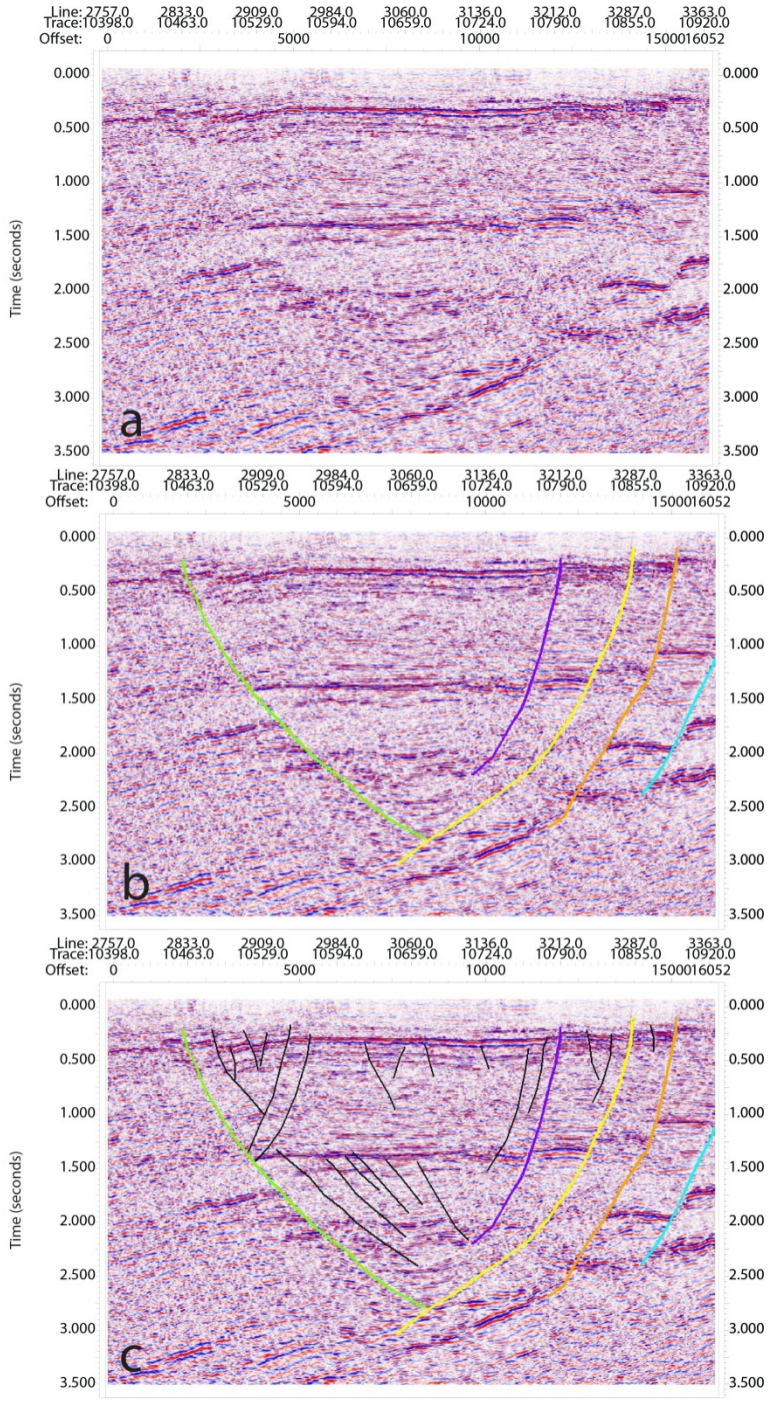

Figure 4. a) Vertical seismic time section without structural interpretation of the NE corner of the reprocessed Balnaves/Haselgrove 3D seismic survey. b) Vertical seismic time section showing an

interpretation of the geometry of the main normal faults used for 3D stress-profile modelling. From L-R the faults are herein termed Ladbroke Grove Fault, NE Fault 1, Pyrus Fault, NE Fault 2, and NE Fault 3. c) Vertical seismic time section showing a full interpretation of faults within the NE Balnaves/Haselgrove 3D seismic survey, Penola Trough. The listric nature of the faults is exaggerated due to the effects of interpretation in the time domain. See Figure 5 for line location.

sections are observed within the top several hundred milliseconds, before shallowing in dip and developing a more listric, moderately dipping character around 1500 milliseconds and deeper. The two main graben-bounding faults, known as the Ladbroke Grove (Figure 4b, green fault) and Pyrus (Figure 4b, yellow fault) faults (Lyon *et al.* 2005b) appear to strike E- W for much of their length. However, east of approximately 483000 both faults appear to have segments that strike in a more NW-SE fashion (Figure 5).

Whilst the major basement-cutting faults extend from depth to the surface, there is a lack of minor faulting in the sediments between 1000 and 1400 milliseconds time (Figure 4c), with small faults occurring both above and below this mark.

Depth conversion of the Balnaves/Haselgrove 3D seismic survey was undertaken using Badleys Trap Tester 6.057. Six wells (Haselgrove-1, Haselgrove South-2, Katnook-1, Katnook-4, Redman-1 and Wynn-1) with checkshot surveys were used for the depth conversion, and were selected for their varied location within the designated modelling area (Figure 1, enlargement). Further fault and horizon interpretation was then performed using Badleys Trap Tester, using the same horizon and fault interpretation techniques described previously.

FAULT REACTIVATION MODELLING

Variations of conditions affecting fault reactivation, such as in-situ stress field orientation, vertical and horizontal stress conditions and rock

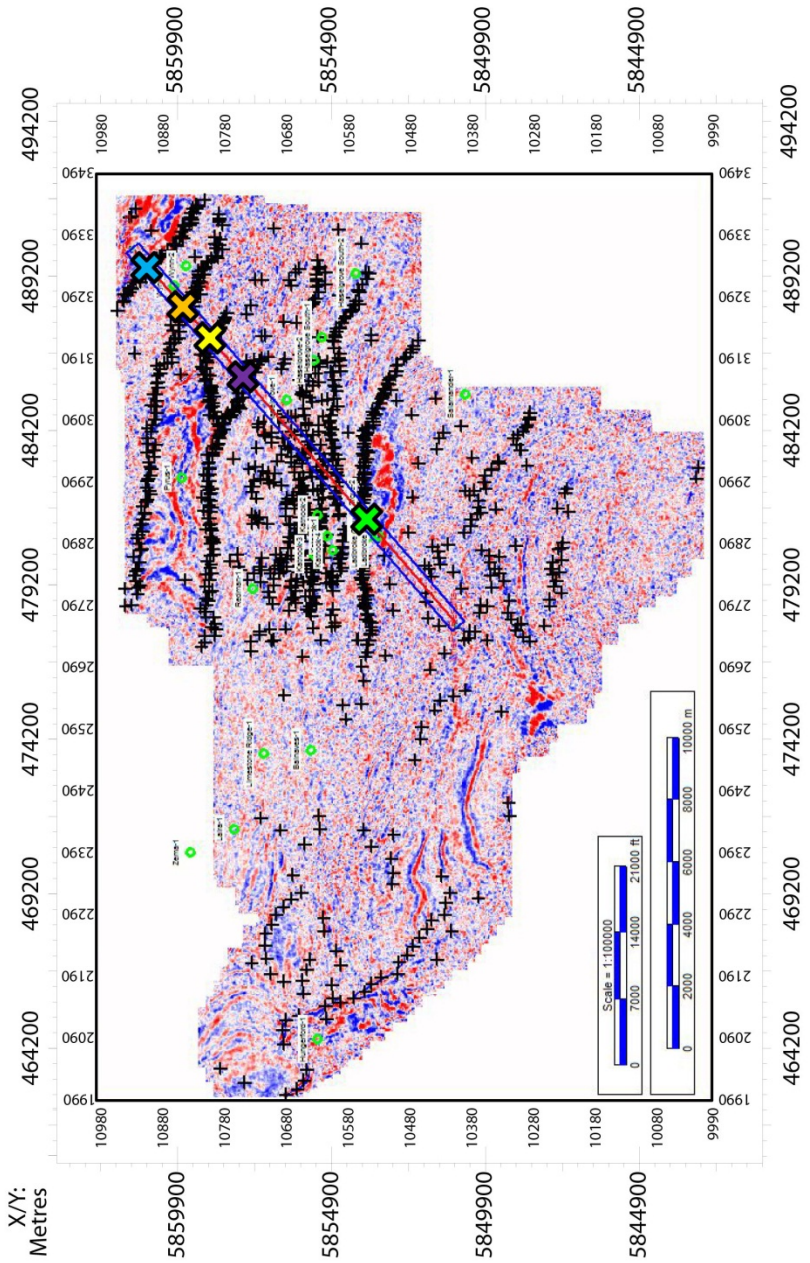

Figure 5. Time slice at 1.78 seconds, showing the focus of interpretation on the northeast section of the survey. The "+" symbols indicate fault cuts at 1.78seconds. The green circles show borehole locations. The red and blue line shows the location of the vertical section in Figure 4. Intersections with the 5 modelled faults (Figure 4b) are indicated by colour coded Xs.

geomechanical properties were used to construct stress profiles (Table 1). Following structural interpretation, seven stress profiles were applied to the modelled faults, displaying three different stress attributes; dilation tendency, slip tendency and fracture stability.

Both dilation and slip tendency models assume a cohesionless surface and depict ratios between zero and one, with higher values equating to a higher likelihood of reactivation. The ratios used were of normalised normal to differential stress and of shear to normal stress for dilation and slip tendency respectively (Figure 6).

Dilation tendency is strongly controlled by resolved normal stress and is able to highlight which fracture orientations are most likely to dilate and hence transmit fluids. Higher dilation tendency values equate to a greater likelihood of fracturing causing dilation and hence a greater ability to allow fluid transmission.

Fracture stability represents the change in pore pressure required to move a fault segment into shear or extensional failure (blue on Figure 6), thus assuming a Griffith-Coulomb failure criterion by giving the fault a value of cohesive strength. This is especially pertinent when referring to cemented cataclasite faults which have significant cohesive strength (Dewhurst *et al.* 2002).

By analysing slip tendency I was able to determine which fault orientations were the most likely to allow slip to occur, and therefore most likely to be associated

Table 1: Values used in the formation of stress attribute displays for each of the seven stress profiles (far-left column). Palaeostress models show age brackets in millions of years ago (Ma). σH, σv and σh represent the maximum horizontal, vertical and minimum horizontal stresses respectively, in megapascals per kilometre (MPa/km). (Jones et al. 2000, Dewhurst & Jones 2002, Dewhurst et al. 2002, Lyon et al. 2005b, Muller et al. 2012).

Stress Profile	σ_H Orientation	σ_H Magnitude (MPa/km)	σ_h Magnitude (MPa/km)	σ_v Magnitude (MPa/km)	Pore Pressure Gradient (MPa/km)	Coefficient of Friction	Coefficient of Internal Friction	Rock Strength (MPa)
Unfaulted Cataclasite	128°	28.7	15.5	21.0	9.8	0.78	0.78	5.44
Unfaulted Reservoir	128°	28.7	15.5	21.0	9.8	0.67	0.67	8.84
Resheared Cataclasite	128°	28.7	15.5	21.0	9.8	0.74	0.74	5.44
Resheared Reservoir	128°	28.7	15.5	21.0	9.8	0.84	0.84	8.84
55Ma	141°	25	20	15	9.8	0.67	0.67	8.84
23-11Ma	136°	25	20	15	9.8	0.67	0.67	8.84
11-6Ma	169°	25	20	15	9.8	0.84	0.84	8.84

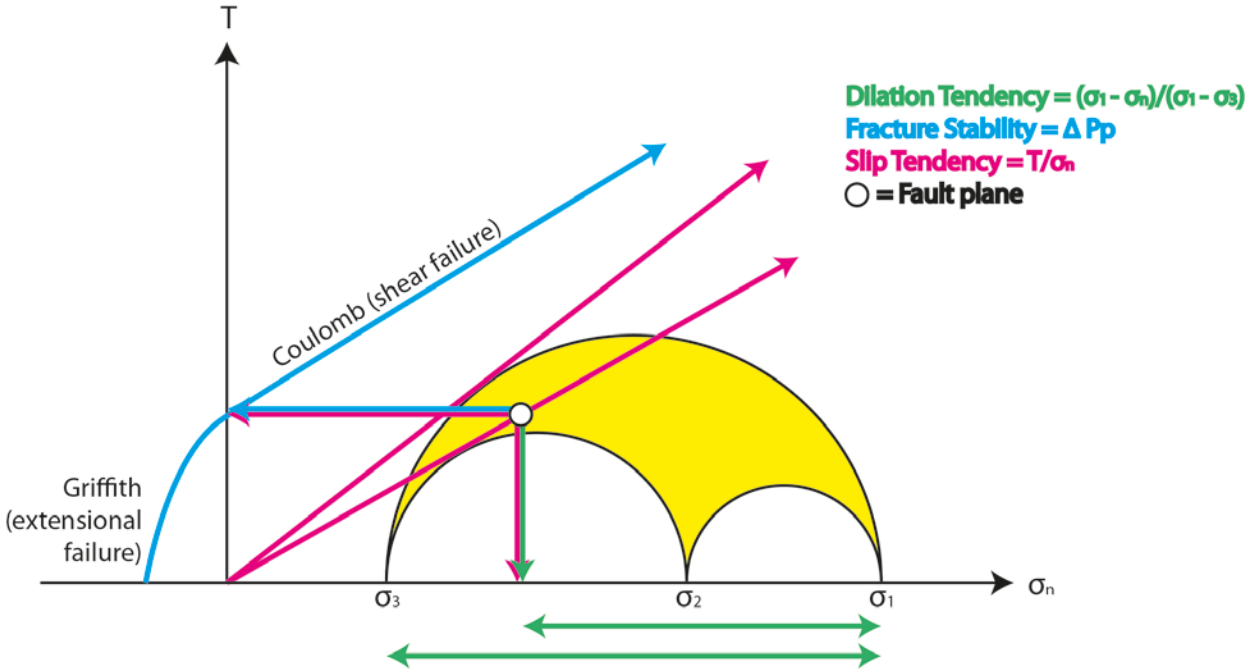

Figure 6. Mohr circle demonstrating the calculations involved with the three different stress attributes modelled in Trap Tester; Dilation Tendency, Fracture Stability and Slip Tendency. T represents shear stress, while σ represents normal stress. The white circle is an example pole to a fault plane. Green arrows indicate the current normal stress value, and the double headed green arrows show the ratio between the normal stress value and the maximum principal stress (σ_1) and the ratio between σ_1 and the minimum principal stress (σ_3), used to determine dilation tendency. The blue arrow shows the Griffith-Coulomb failure criterion, which indicates the change from current pore pressure (ΔPp) at the pole to the plane needed to cause shear or extensional failure. Pink arrows show the values of shear and normal stresses exerted at that fault location, as well as the current slip tendency (stable) and the slip tendency at which beyond the pole would be unstable (σ_2 represents the intermediate principal stress) (Figure after Cosgrove (1998)).

with enhanced permeability. The higher the slip tendency ratio, the greater the likelihood that the fault will slip by shear fracturing. Slip usually begins when the ratio is equivalent to the coefficient of static friction.

Applying the stress profiles to the modelled faults allowed a visual representation of the stress attributes to be displayed and assessed. A complete method of stress profile construction and modelling can be found in Appendix A.

FAULT REACTIVATION IN THE PENOLA TROUGH

FAULT REACTIVATION DATA LIMITATIONS

When modelling fault planes, lateral lithology heterogeneity can affect the sealing potential of faults. This may indeed play a role in the presence of an intact hydrocarbon column on the NW-SE striking Haselgrove field. While well control enables accurate analysis close to boreholes, increasing distance between well controls gives rise to interpolation uncertainty, as well as extrapolation uncertainty when moving away from any well control (Gluyas & Swarbrick 2004).

Palaeostress models used arbitrary stress magnitudes in their calculations, which were similar to today's magnitudes, and were applied to a modelled stress regime. As such, the results obtained will not be completely accurate. They are, however, good representations of the past stress regimes, and because of this the results can be analysed with a degree of certainty that they are somewhat accurate.

FAULT REACTIVATION MODEL RESULTS

Present-Day Stress Profile Models

The results show that depth does not influence dilation or slip tendency; however increasing the depth results in the effective stress being decreased, lowering the pore pressure needed to move the fault plane into failure and resulting in changes to fracture stabilities (Figure 7).

To tailor the results towards industry applications, Mohr Circle diagrams were constructed for a depth of 2500 metres, which was chosen due to its general proximity across the trough to the Pretty-Hill sandstone, which acts as a reservoir within the Otway Basin (Dewhurst *et al.* 2002). These models were relevant for hydrocarbon exploration, CO_2 sequestration and geothermal energy plays (Stevens *et al.* 2001, Boult & Hibburt 2002).

DILATION TENDENCY MODELS

Dilation tendency models for all present-day rock types yield similar results (Figures 8a, 9a, 10a, 11a). Fault segments striking E-W generally have dilation ratios of between 0.4 and 0.6, depending on fault plane roughness, and irrelevant of dip. However, fault segments striking in a NW-SE fashion have ratios upwards of 0.8 at shallow depths where fault dip is steep. By approximately 2500m depth the fault is sufficiently shallowed in dip so as to have ratios ranging from 0.5 to 0.7.

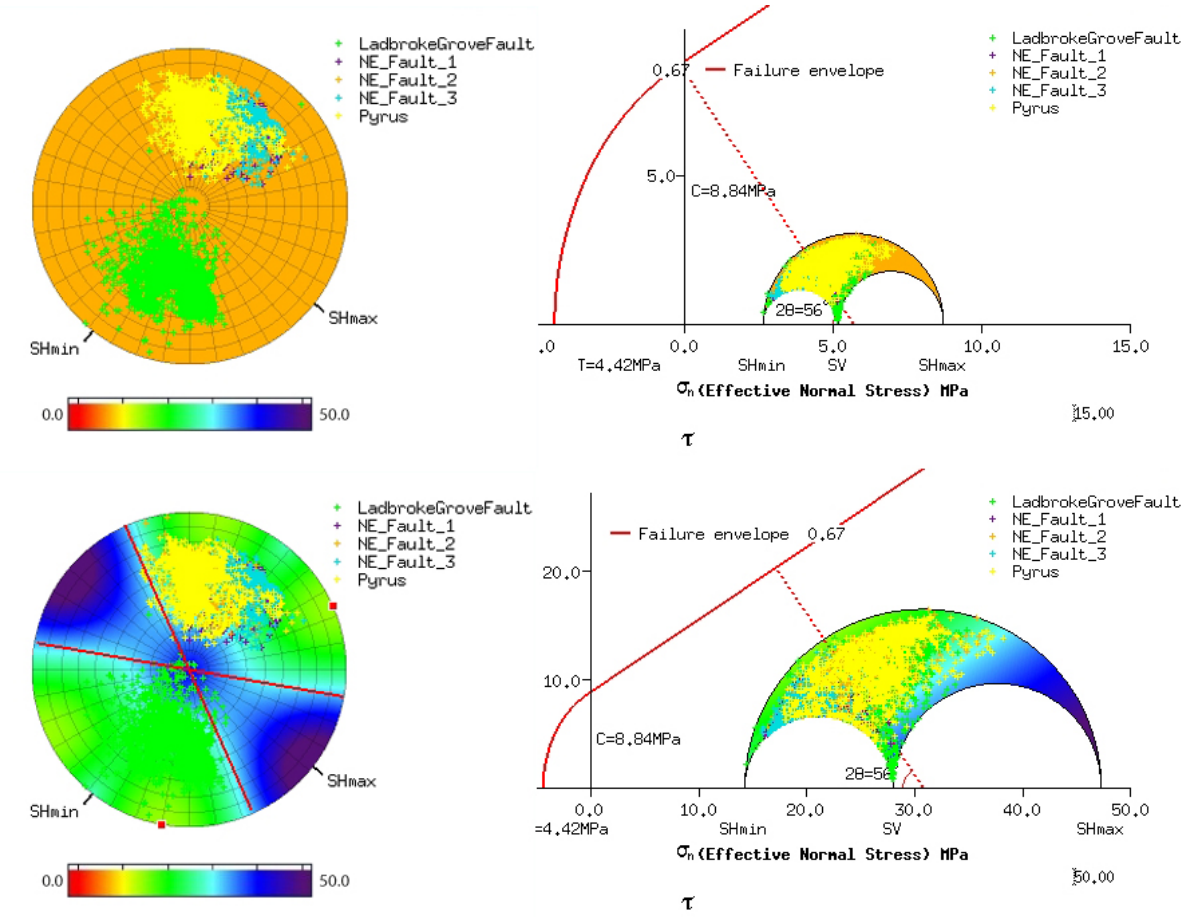

Figure 7: Comparison of present-day fracture stabilities of unfaulted reservoir rock at different depths. Top stereogram and Mohr Circle Diagram show fracture stabilities at 460m depth. Bottom stereogram and Mohr Circle Diagram show fracture stabilities at 2500m depth. SHmin and SHmax show the orientations of the minimum and maximum horizontal stresses respectively. The colour scale is showing the change in pore pressure (in megapascals, MPa) needed to move the fault plane into failure. The Y axis of the Mohr Circle Diagrams shows the shear stress, T.

FRACTURE STABILITY MODELS

Fracture stability models appear to show highest stability values at the bottom of interpreted faults, where dip is shallowest; often needing changes in pore pressure of 40 to 50MPa to cause fault planes to become unstable (Figures 8b, 9b, 10b, 11b). For the most part there is an almost linear increase in fracture stability with depth, save for a section where there appears to be a sharp jump in values. These jumps of approximately 5MPa occur at 824-825m in cataclasite models and at 1339-1340m in reservoir models.

FAULT REACTIVATION IN THE PENOLA TROUGH

SLIP TENDENCY MODELS

Slip tendency models (Figures 8c, 9c, 10c, 11c) give similar results to that of dilation tendency. All present-day lithologies are almost identical, with high end slip tendency ratios of 0.4 to 0.5 found at the top of faults where dip is steepest. These higher ratios are predominantly found on E-W striking fault segments. Like most of the dilation tendency models, the lowest slip tendency ratios (0.1 – 0.2) are found on moderately dipping fault segments.

Palaeostress Models

Rock strength data used for the palaeostress models was varied based upon two assumptions. Firstly, it was assumed that reservoir rock between 55 and 11Ma was unfaulted, and secondly that reservoir rock in the period 11-6Ma would be undergoing a successive stage of reactivation.

DILATION TENDENCY PALAEO-MODELS

All palaeo-models of dilation tendency (Figures 12a, 13a, 14a) gave results with higher ratios of up to 0.9 at depths below the Pretty Hill Sandstone, and especially so on fault segments at depth striking NW-SE. The reverse is found above the Pretty Hill Sandstone, with higher ratios found on E-W striking segments than NW-SE striking segments. Overall, there was a negligible decrease in dilation tendency ratios from 55Ma (Figure 14a) to 23-11Ma (Figure 13a), before a uniform increase in ratios by around 0.1 from 23-11Ma (Figure 13a) to 11-6Ma (Figure 12a).

FAULT REACTIVATION IN THE PENOLA TROUGH

FRACTURE STABILITY PALAEO-MODELS

Models of palaeostress fracture stability (Figures 12b, 13b, 14b) are alike for all palaeostress regimes, with minimal change from 55Ma (Figure 14b) to 23-11Ma (Figure 13b), and a small increase in stability from 23-11Ma (Figure 13b) to 11-6Ma (Figure 12b). All regimes show changes in pore pressure of approximately 10MPa needed to cause fault reactivation from the surface until around the depth of the Laira Formation. Again, like present-day stress regimes, we see a 10MPa "jump" in values at this depth. Below this, most values hover around 20MPa needed to cause reactivation, regardless of strike. The shallowest-dipping parts of the faults show the highest levels of fracture stability, needing a 40MPa change in pore pressure to cause fault instability in some segments. Palaeostress models often appear to be less stable at depth than present day findings.

SLIP TENDENCY PALAEO-MODELS

Slip tendency palaeo-models (Figures 12c, 13c, 14c) show that where dips are shallower, high (~0.5) ratios are often found. In NW-SE striking fault segments, these high-end ratios occur below Pretty Hill Sandstone depths, for all palaeostress models. For the most part, lower ratios of between 0.3 and 0.4 are found above the Pretty Hill Formation. However, these low ratios extend to depth on fault segments striking E-W in the most recent palaeostress model, 11-6Ma (Figure 12c). Overall, slip tendency ratios oppose that of dilation tendency; a slight increase in slip tendency occurs between 55Ma (Figure 14c) and 23-11Ma (Figure 13c), before a large decrease in slip tendency ratio of 0.1-0.2 from 23-11Ma (Figure 13c) to 11-6Ma (Figure 12c).

FAULT REACTIVATION IN THE PENOLA TROUGH

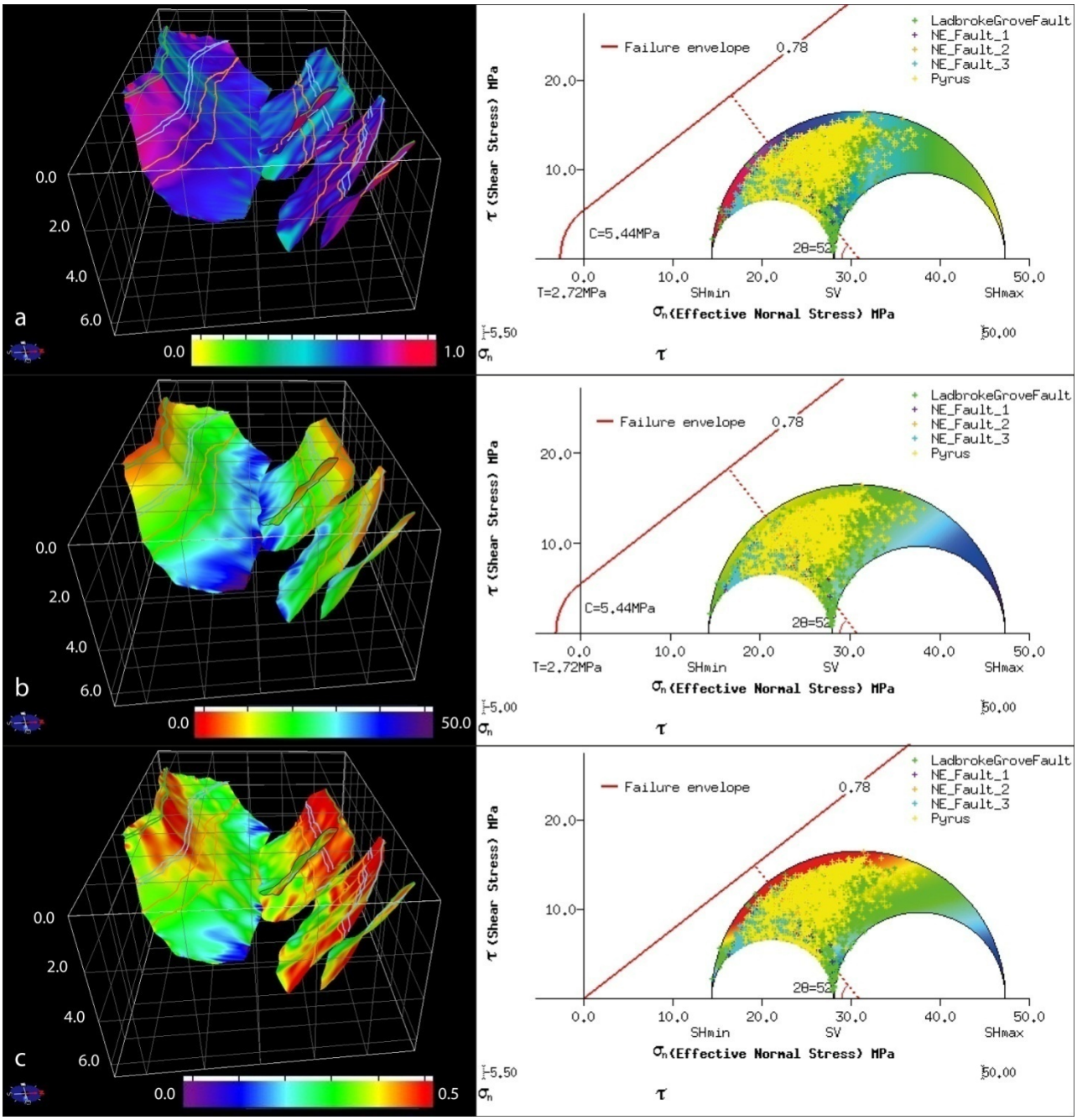

Figure 8. 3D model and related Mohr Circle of present-day unfaulted cataclasite rock coloured for a) Dilation tendency b) Fracture stability c) Slip tendency. Green lines on modelled fault planes show the position of Pebble Point Formation hanging and footwall locations. Blue lines show the position of Laira Formation hanging and footwall locations. Orange lines show the position of Pretty Hill Formation hanging and footwall locations. 3D model grid increments are every 2 kilometres.

FAULT REACTIVATION IN THE PENOLA TROUGH

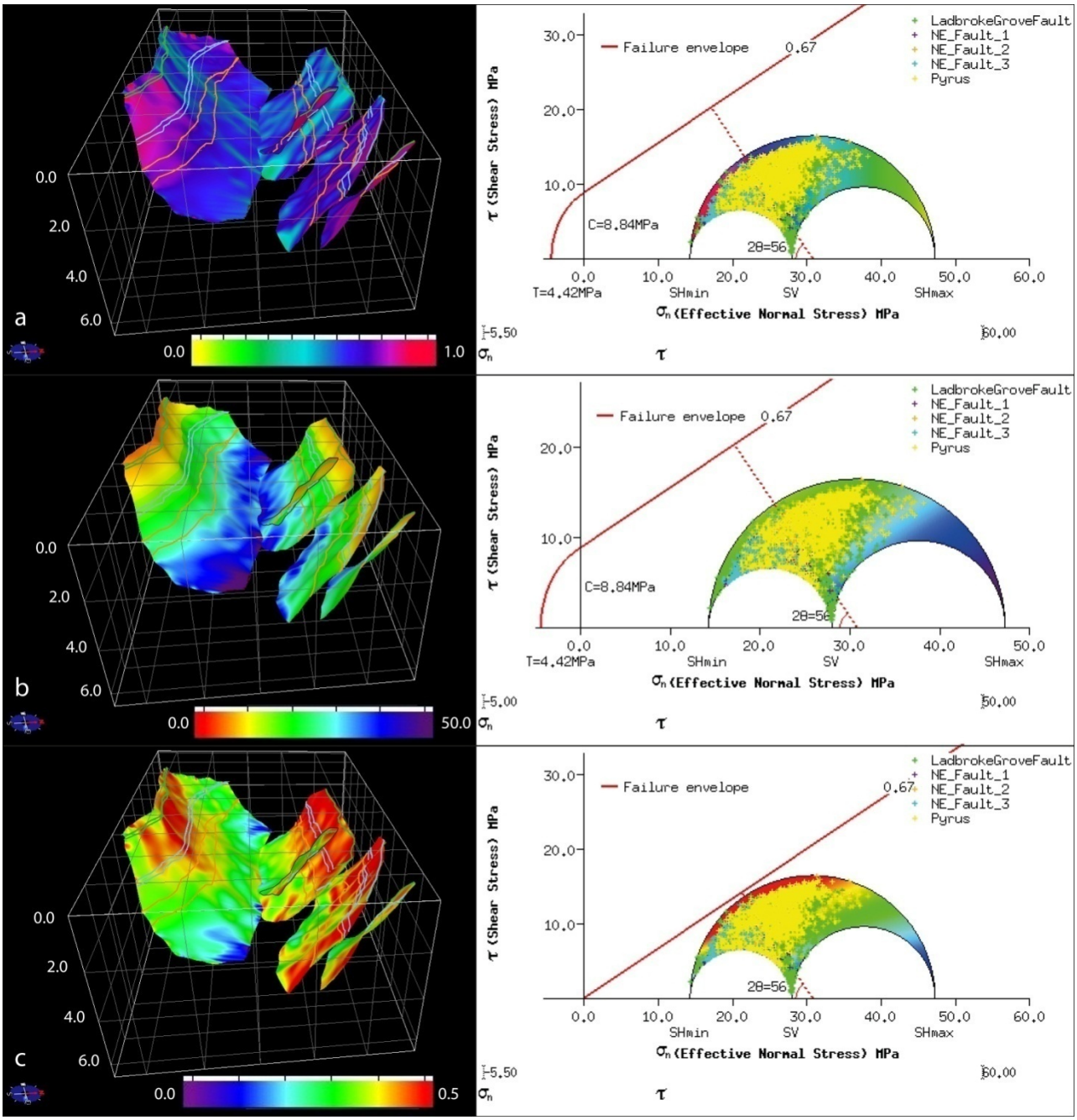

Figure 9. 3D model and related Mohr Circle of present-day unfaulted reservoir rock coloured for a) Dilation tendency b) Fracture stability c) Slip tendency. Green lines on modelled fault planes show the position of Pebble Point Formation hanging and footwall locations. Blue lines show the position of Laira Formation hanging and footwall locations. Orange lines show the position of Pretty Hill Formation hanging and footwall locations. 3D model grid increments are every 2 kilometres.

FAULT REACTIVATION IN THE PENOLA TROUGH

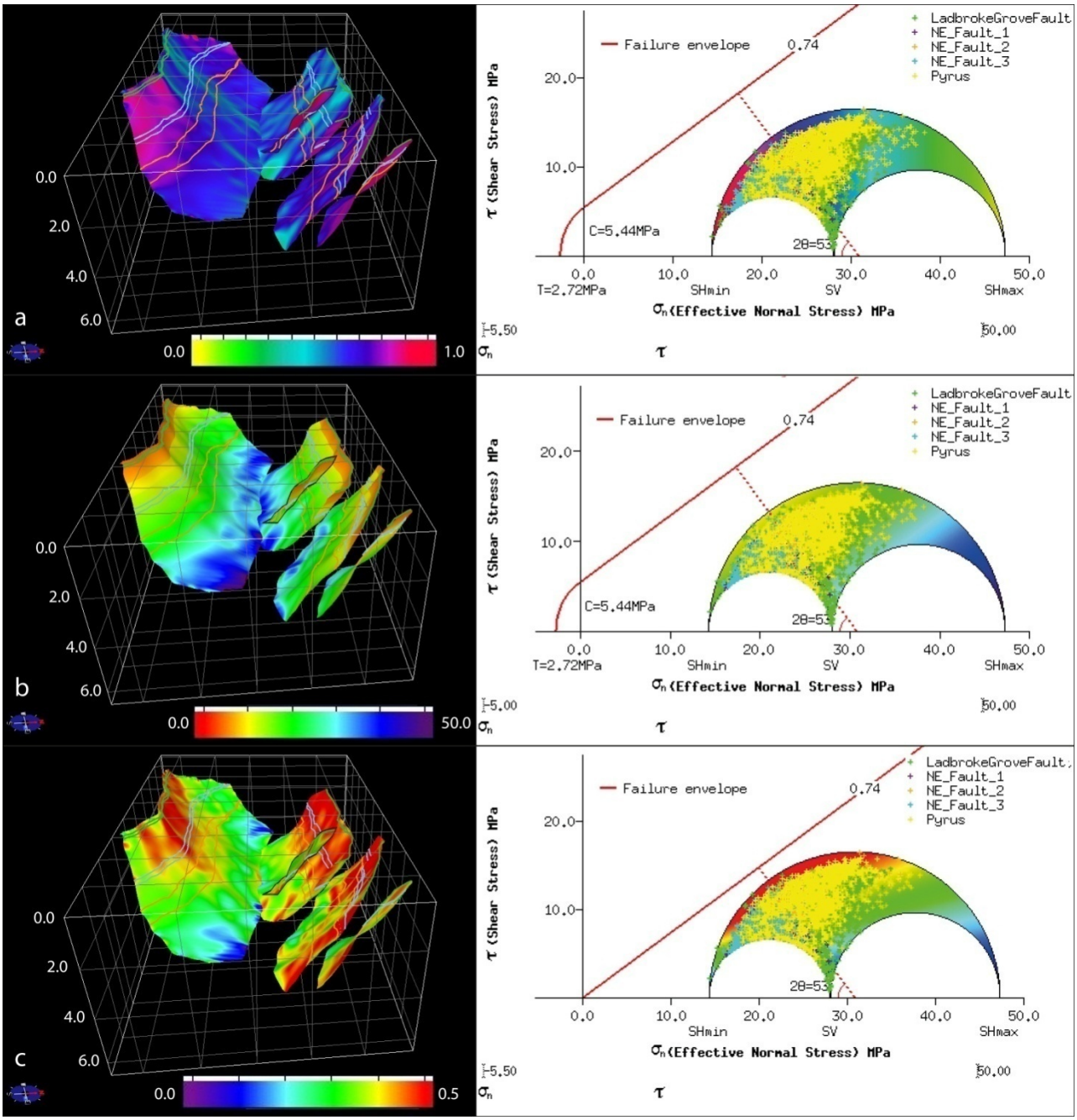

Figure 10. 3D model and related Mohr Circle of present-day resheared cataclasite rock coloured for a) Dilation tendency b) Fracture stability c) Slip tendency. Green lines on modelled fault planes show the position of Pebble Point Formation hanging and footwall locations. Blue lines show the position of Laira Formation hanging and footwall locations. Orange lines show the position of Pretty Hill Formation hanging and footwall locations. 3D model grid increments are every 2 kilometres.

FAULT REACTIVATION IN THE PENOLA TROUGH

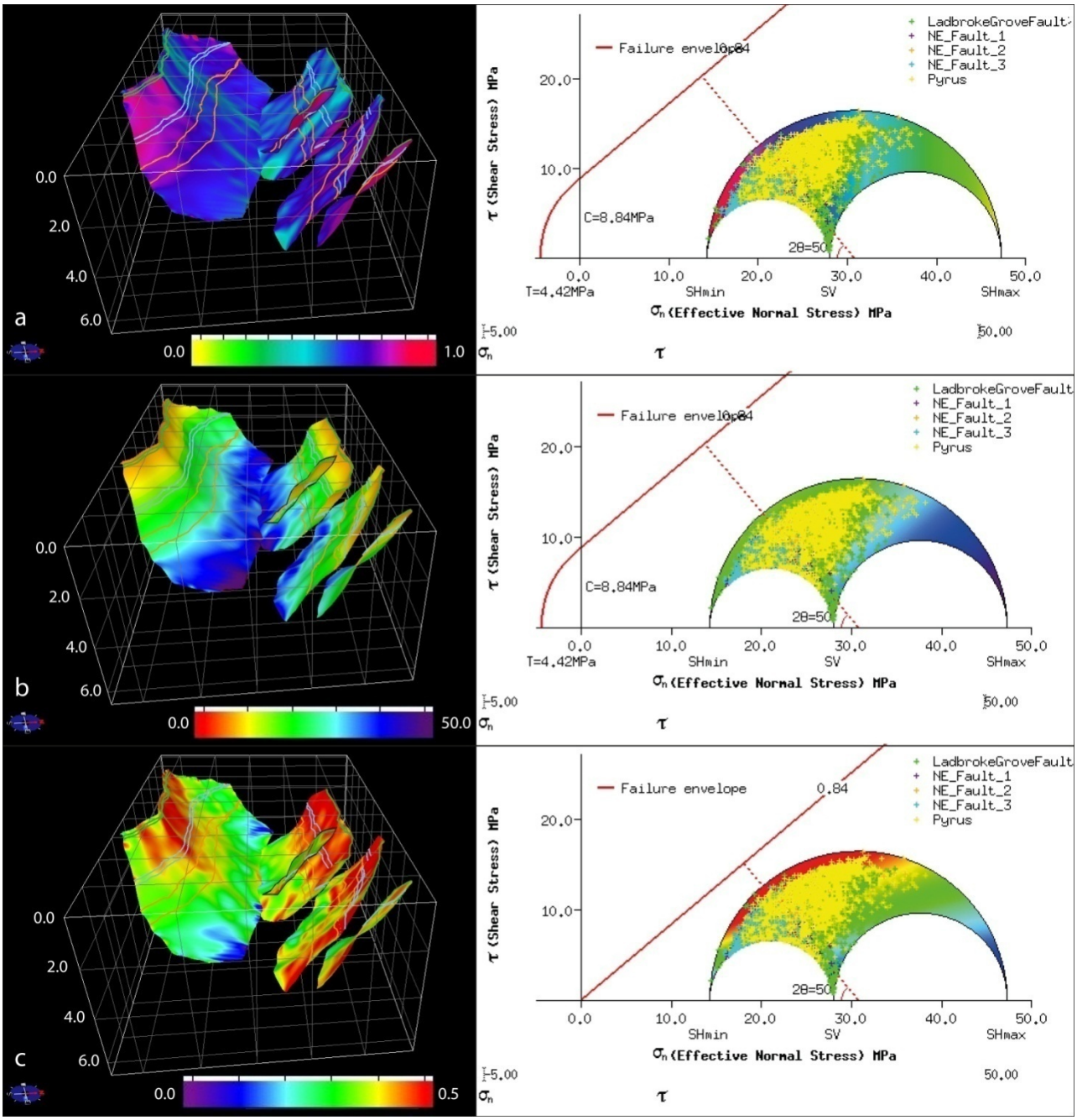

Figure 11. 3D model and related Mohr Circle of present-day resheared reservoir rock coloured for a) Dilation tendency b) Fracture stability c) Slip tendency. Green lines on modelled fault planes show the position of Pebble Point Formation hanging and footwall locations. Blue lines show the position of Laira Formation hanging and footwall locations. Orange lines show the position of Pretty Hill Formation hanging and footwall locations. 3D model grid increments are every 2 kilometres.

FAULT REACTIVATION IN THE PENOLA TROUGH

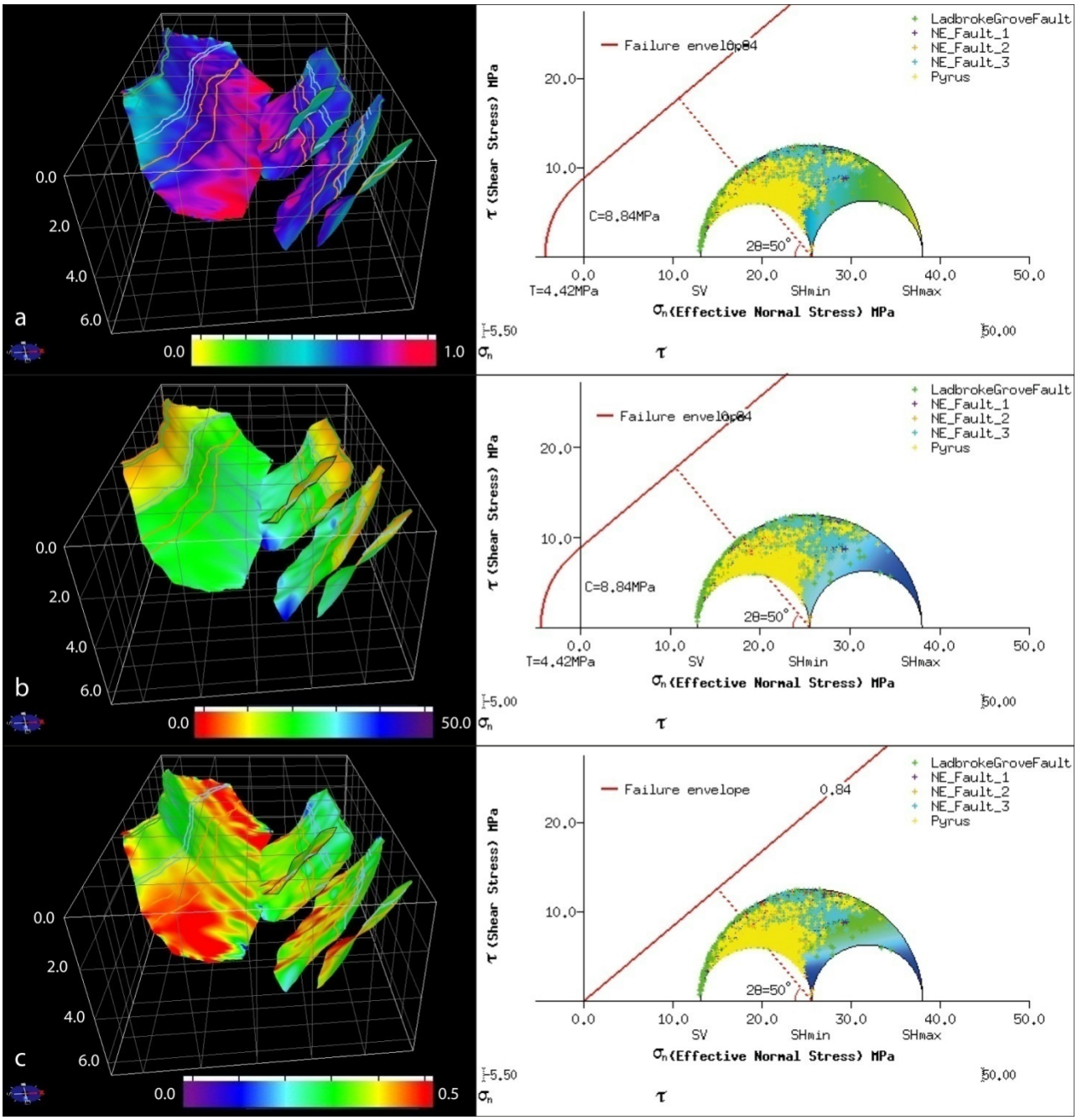

Figure 12. 3D model and related Mohr Circle of resheared reservoir rock from 11-6Ma coloured for a) Dilation tendency b) Fracture stability c) Slip tendency. Green lines on modelled fault planes show the position of Pebble Point Formation hanging and footwall locations. Blue lines show the position of Laira Formation hanging and footwall locations. Orange lines show the position of Pretty Hill Formation hanging and footwall locations. 3D model grid increments are every 2 kilometres.

FAULT REACTIVATION IN THE PENOLA TROUGH

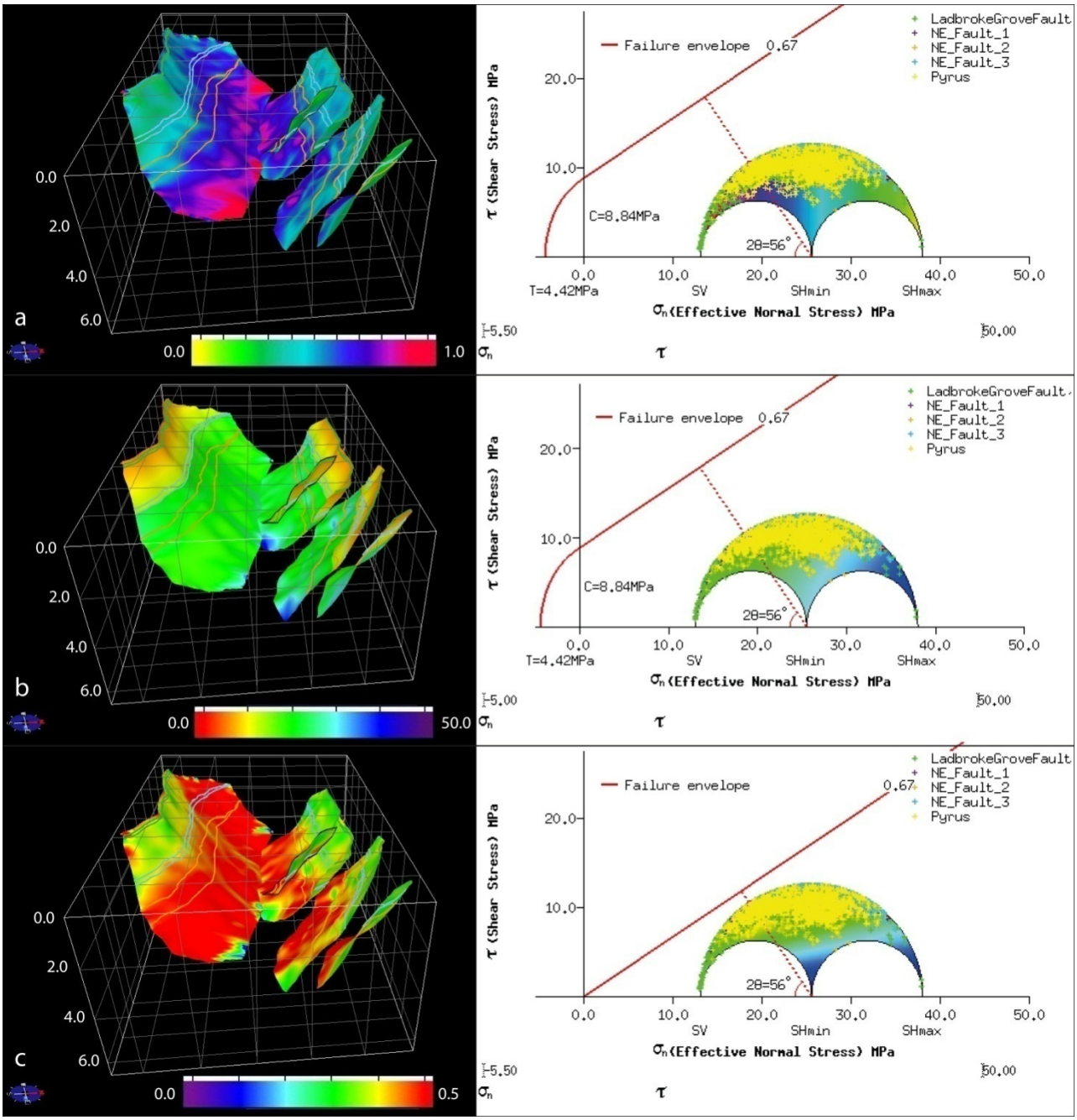

Figure 13. 3D model and related Mohr Circle of unfaulted reservoir rock from 23-11Ma coloured for a) Dilation tendency b) Fracture stability c) Slip tendency. Green lines on modelled fault planes show the position of Pebble Point Formation hanging and footwall locations. Blue lines show the position of Laira Formation hanging and footwall locations. Orange lines show the position of Pretty Hill Formation hanging and footwall locations. 3D model grid increments are every 2 kilometres.

FAULT REACTIVATION IN THE PENOLA TROUGH

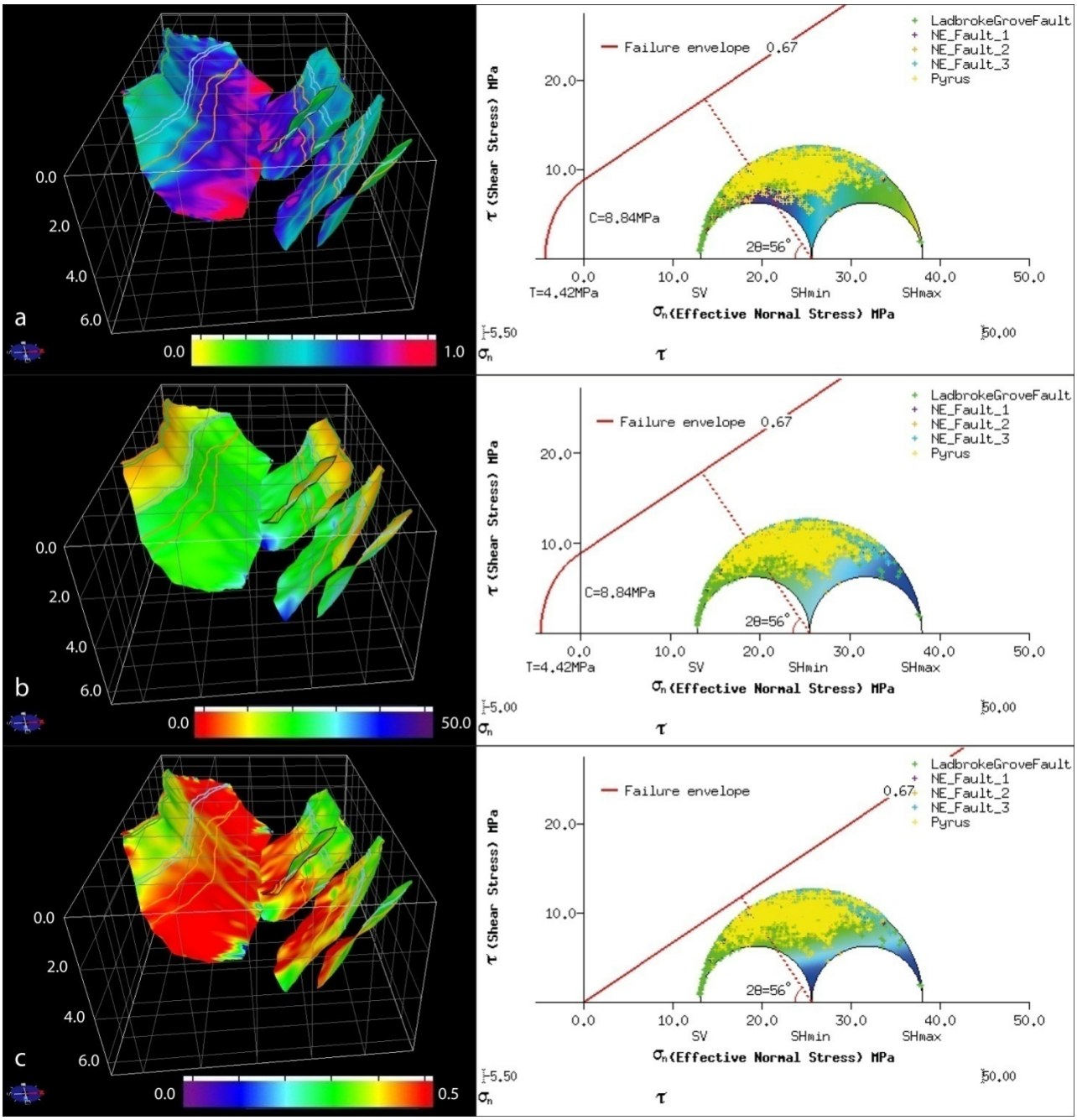

Figure 14. 3D model and related Mohr Circle of unfaulted reservoir rock from 55Ma coloured for a) Dilation tendency b) Fracture stability c) Slip tendency. Green lines on modelled fault planes show the position of Pebble Point Formation hanging and footwall locations. Blue lines show the position of Laira Formation hanging and footwall locations. Orange lines show the position of Pretty Hill Formation hanging and footwall locations. 3D model grid increments are every 2 kilometres.

DISCUSSION

Balnaves/Haselgrove 3D Seismic Interpretation

While some of the fault dip shallowing can be attributed to the velocity effects associated with interpreting in the time domain (Gluyas & Swarbrick 2004), a large proportion of the character is assumed to be from genuine listric faults associated with the normal faulting of the area, due to the slightly listric shape of the faults following depth conversion.

Interpretation of the seismic data reveals a normal fault regime, with some evidence of compressional structures in the form of minor anticlines. Thicker sediment packages in the hanging wall reveal that syn-rift sedimentation was occurring during the deposition of several sedimentary units. This is more pronounced at depth where units are thicker, demonstrating more movement along faults during deposition of deeper units, or alternatively a lower depocentre during deposition. Different stress regimes are revealed by fault sets striking both E-W and NW-SE, as demonstrated by the changing in fault strike of both major and minor faults.

The changing fault strike of the graben-bounding Ladbroke Grove fault and the strike of NE Fault 1 (Figure 5) represent a change in formation mechanism or localised stress regime between the formation of these faults and later faults. Boult *et al.* (2008) refer to the NNW-SSE striking Hungerford-Kalangadoo and St. George faults (Boult *et al.* 2008) as being formed along pre-existing Cambrian basement weaknesses prior to the

formation of younger E-W striking faults. It is possible that the location and trend of the NW-SE striking portion of the Ladbroke Grove fault and NE Fault 1 were influenced by pre-existing basement weaknesses in the same style as the Hungerford-Kalangadoo and St. George faults. An early NE-SW oriented extensional direction may also have played a part in their formation. During subsequent N-S directed rift extension, weaknesses in the surrounding rock may have concentrated the fault formation to then propagate in a more E-W striking direction from the tail end of the earlier NW-SE striking faults. The NE Fault 1 appears to splay from the more dominant Pyrus Fault, and the proximity of the two may be caused by the change in palaeostress regime.

During the Aptian and Albian, a period of sag rifting often associated with faulting quiescence was acting upon the Otway Basin, as witnessed in the Penola Trough (Boult *et al.* 2008). Faults above the 1000 millisecond mark (Figures 4c, 15) are often minor, and can strike NW-SE. This suggests that their method of formation differs from that which caused the major E-W striking basement-cutting faults to form (Boult *et al.* 2002). The primary difference between these two fault sets is the in-situ palaeostress regime. During the deposition of sediments below 1000 milliseconds the maximum horizontal palaeostress direction was oriented for N-S extension, causing predominantly E-W striking faults. However, during the period of sedimentation above 1000 milliseconds, the palaeostress was oriented for NE-SW extension (Boult *et al.* 2008) causing the minor NW-SE trending faults (Figure 15).

FAULT REACTIVATION IN THE PENOLA TROUGH

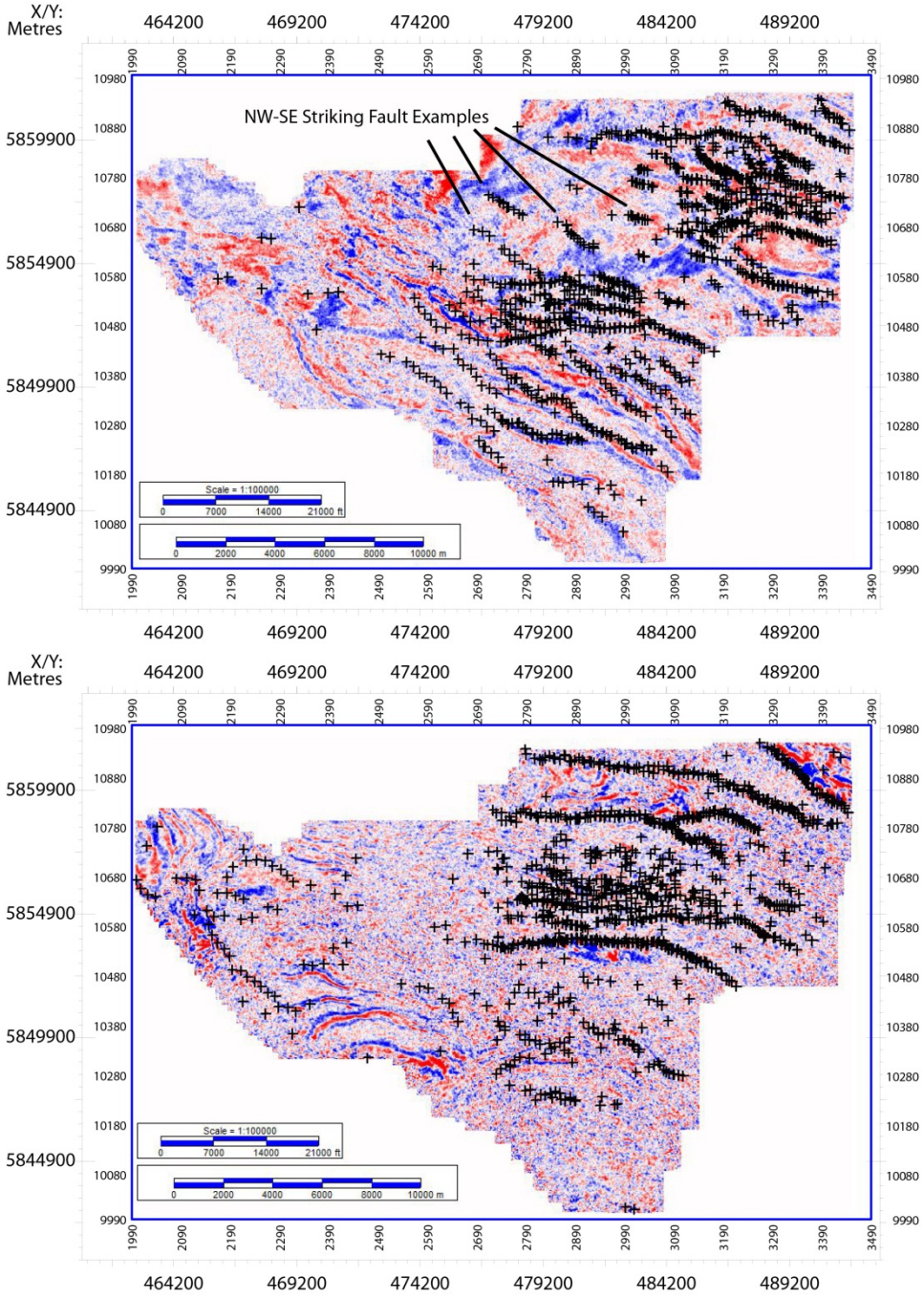

Figure 15: Time slice comparisons of faults at 0.45 (top) and 1.75 (bottom) seconds, showing a focus on fault interpretation within the area chosen for modelling. Minor faults a t 1.75 seconds appear to be preferentially oriented E-W, while at 0.45 seconds there is a higher likelihood of faults striking NW-SE as indicated.

FAULT REACTIVATION IN THE PENOLA TROUGH

The validity of steeply dipping listric S-SSW and N-NNE dipping normal faults that extend from the surface to approximately 3 seconds of time, where they offset basement rock, is supported by many previous works (Boult *et al.* 2004, Lyon *et al.* 2004, Lyon *et al.* 2005a, Boult *et al.* 2008, Camac & Hunt 2009). These authors reinforce the strength of the interpretation herein with faults of a similar location, spacing, strike and dip (Boult *et al.* 2004, Boult *et al.* 2008). Lyon *et al.* (2004) present seismic interpretation results in the time domain, as well as depth domain, which show listric faults in the time domain becoming more planar in the depth domain, as predicted and observed in this project's interpretation.

Seismic interpretation demonstrates that the Penola Trough has analogous structural styles to extensional basins around the world. Finlayson *et al.* (1996) compare the Late Cretaceous faulting in the Otway Basin with the extensional basins of the North Sea margin of NE United Kingdom, also noting that, like the Otway Basin, pre-existing structures played a part in the geometry of rifting. The basins of the NE United Kingdom are also comparable to the Otway Basin, both possessing similar ages of rifting and proximity to the margin, as well as Cenozoic inversion structures (Williams *et al.* 2005, Holford *et al.* 2009).

Differences between aforementioned interpretations and this project's interpretation come with respect to the smaller features, which are more susceptible to interpreter error due to seismic resolution reasons (Gluyas & Swarbrick 2004). The interpretation herein

differs slightly from other authors' interpretations (e.g. Lyon *et al.* 2007) around the Ladbroke Grove fault (Figures 4b, 4c and 5). Interpretations by Lyon *et al.* (2007) show minor antithetic faults extending from the Ladbroke Grove fault, truncating smaller northward dipping faults (Lyon *et al.* 2007). The interpretation herein could not connect the minor faults found within this area (Figure 4c) with either of the graben-bounding faults with a large enough degree of certainty so as to ensure their authenticity. The differences between final interpretations could be attributed to an area of poor resolution associated with diffraction and fault shadowing associated with the numerous faults in the graben interior.

The hypothesis that faults striking NW – SE in the Penola Trough, Otway Basin, would allow fluid flow under the in-situ stress regime was primarily supported by the presence of large faults that do strike NW-SE. Although most of the main faults strike in a more E-W fashion they were still analysed for reactivation likelihood.

3D Fault Reactivation Modelling

The similarity of results obtained for each lithology, be it for dilation tendency, slip tendency or fracture stability, support a conclusion in which rock data does not control reactivation likelihood to a large degree. Stress magnitudes and orientations are therefore the probable primary cause of any reactivation likelihood changes.

The sudden jump in pore pressure values required to cause failure demonstrated in fracture stability models represents a change in failure mode. Above this point the maximum possible shear stress is less than the cohesive strength, meaning that the

material cannot fail by shear, and leaving tensile failure as the only possible failure mechanism. Below the "jump", the maximum possible shear stress is larger than the cohesive strength, meaning that fracture stability varies depending on fault orientation alone.

All in-situ stress regimes show that the NW-SE striking fault segments are equal to or more likely to dilate than E-W striking segments, regardless of fault dip, supporting the overarching hypothesis that faults striking NW – SE in the Penola Trough, Otway Basin, will allow fluid flow under the in-situ stress regime. Present-day slip tendencies and fracture stabilities seem to rely on dip or depth rather than strike, with steeper dipping segments displaying higher slip tendencies and appearing more prone to fracturing than moderately dipping segments. Therefore, NW-SE striking fault segments, generally at depths from between the Pretty Hill and Laira formations and above, appear to be most prone to reactivation under the present-day stress conditions. This finding provides additional information to the original hypothesis, enabling us to define a dip (steep) as well as a strike most likely to reactivate for the faults in question. Palaeostress conditions show a different scenario, however.

In all palaeostress age brackets modelled in this study, dilation tendencies are highest at deep depths (~2500m), regardless of strike (Figures 12a, 13a, 14a), which is almost a complete reversal to today's conditions. Likewise, slip tendencies are highest at depth, especially so in NW-SE striking segments, but show the lowest ratios on shallow fault

segments, especially those striking E-W. There is an overall decrease in slip tendency from 55Ma to present-day, but an increase in dilation tendency. This may be attributed to a decrease in shear stress, or a small increase in normal stress coupled with a large increase in horizontal maximum stress. Fracture stability again shows the most unstable faults to be shallow and steep dipping, with fault strike not affecting results.

When comparing the palaeostress models of different ages, a negligible change in dilation and slip tendencies from 55Ma to 23-11Ma is observed, as well as a larger change from 23-11Ma to 11-6Ma. Present-day models demonstrate that lithology characteristics play little role in the reactivation likelihood. If this is a valid conclusion, then varying the stress field would result in more noticeable changes to the reactivation models. Modelled present day in-situ stress orientations compare well with measured in-situ stress orientations, showing a mean residual misfit of 12°, indicating the accuracy level of the palaeostress orientations. The σ_H orientation at 55Ma was oriented towards N141°E before moving anticlockwise to be at N136°E by 23-11Ma and finally underwent a large clockwise change to N169°E by 11-6Ma (Muller *et al.* 2012). The small σ_H orientation change (only 5°) from 55Ma to 23-11Ma would have brought about the small changes in models seen in that time bracket; whilst the large clockwise change (33°) would have given rise to the larger change in various reactivation likelihoods in the period from 23-11Ma to 11-6Ma.

Palaeostress results suggest that at 55Ma, deep NW-SE striking faults were most prone to reactivation, followed by shallow NW-SE striking faults and E-W striking faults. From that stage to the present day, there was an overall increase in likelihood of dilation, and a minimal decrease in fracture stability, both of which were countered by a decrease in likelihood of slip. This change from the past to the present-day supports the additional hypothesis in which a changing stress field will give rise to changing reactivation likelihoods.

Relevance to hydrocarbon exploration

Hill and Boult (2002b) present the main local hydrocarbon source rocks as being the Casterton Formation, an unnamed basal shale of the Pretty Hill Formation, the Sawpit shales and Laira and Eumeralla formations (Figure 2). Of these, maturation levels and depths have been calculated by Hill and Boult (2002a) (Table 2), leaving the Pretty Hill Formation, Sawpit shales, unnamed basal shales and the Laira and Casterton formations between 1900 and 3800 metres depth to be the prime exploration candidates due to their maturity levels.

Lovibond *et al.* (1995) used burial history modelling to determine a generation timing of hydrocarbons, pointing towards an Early Cretaceous generation time. This implied that hydrocarbons in the Penola Trough migrated vertically following the Early Cretaceous (Lovibond *et al.* 1995). Hydrocarbon migration was assumedly facilitated by the same faults and carrier beds by which Lovibond *et al.* (1995) assume allowed CO_2 to charge the Ladbroke Grove Field. Duddy *et al.* (2003) note that migration of

hydrocarbons in the offshore Morum Sub-basin began during the Late Cretaceous, reiterating Lovibond *et al.*'s migration timings to a degree. However, this timing is likely to be different than that of migration in the Penola Trough.

Table 2. Maturity modelling of areas in proximity to the Balnaves/Haselgrove 3D seismic survey, showing the maturities as classified by the depth in metres below kelly-bushing (m KM) and maximum vitrinite reflectance ($R_v$max). The Sawpit area is located 10km to the north of the modelled faults (from Hill and Boult (2002a)).

Location	Depth (m KB)	R_v max	Maturity Level	Unit
Sawpit area	1350	0.5	Early mature (oil)	Laira, Pretty Hill
Katnook area	1700	0.5	Early mature (oil)	Lower Eumeralla, Windermere Member, Katnook, Laira
Sawpit area	1900	0.7	Mid mature (oil)	Basal Pretty Hill, Sawpit Shales, unnamed basal shales, Casterton
Katnook area	2300	0.7	Mid mature (oil)	Laira
Katnook area	3050	1.0	Late mature (oil)	Pretty Hill
Katnook area	3800	1.3	Main gas generation	Basal Pretty Hill, Sawpit Shales, unnamed basal shale, Casterton
Katnook area	5200	2.6	Overmature	Basal Casterton

Comparison of palaeostress models, hydrocarbon maturities and migration timings allowed analysis of likely hydrocarbon traps. Figure 16 shows the locations of known present and past hydrocarbon accumulations within the modelled area. Most main gas accumulations are or were located on E-W striking fault traps, except the Haselgrove play, which is located on a NW-SE striking fault (Lyon *et al.* 2004). This could be due

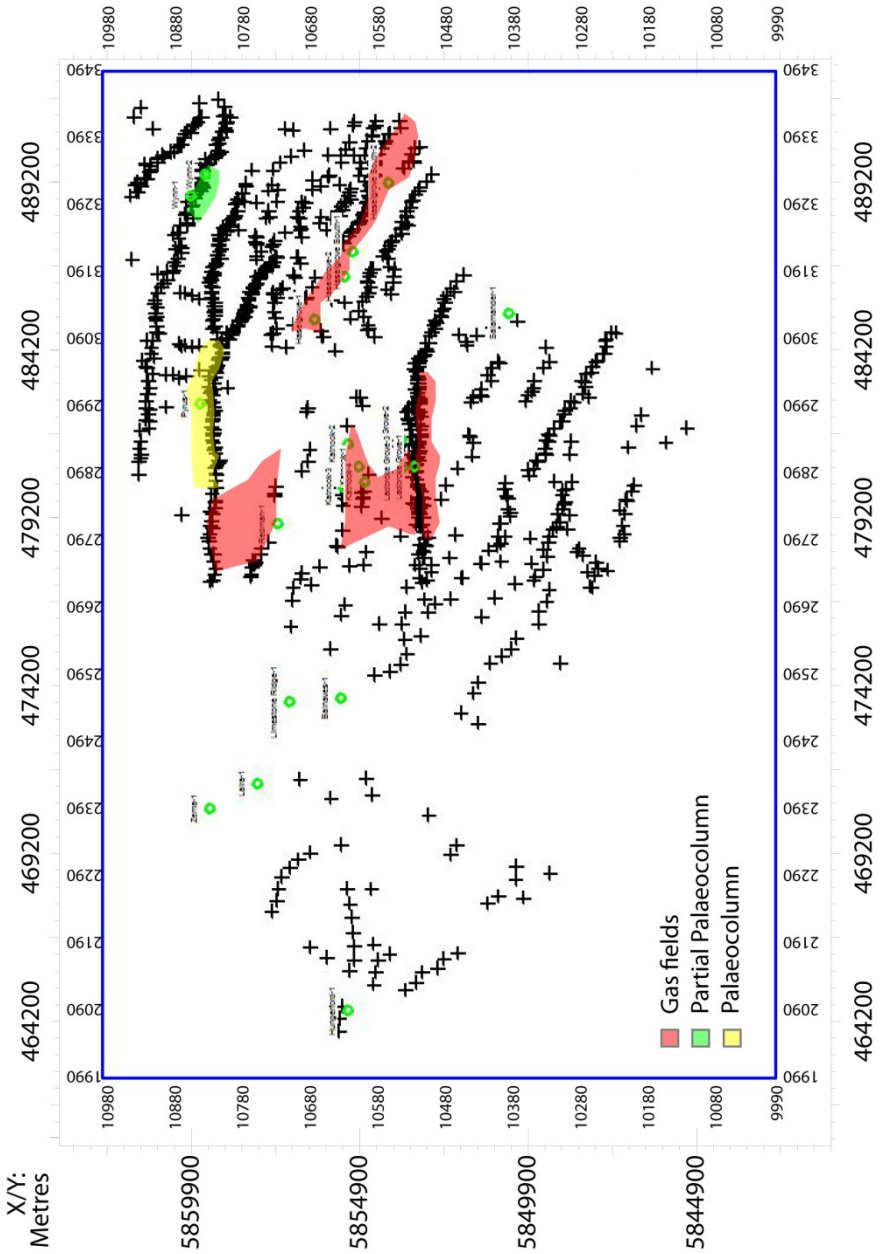

Figure 16. Time slice at 1.78 s ccumulations within the mo(green circles). Red areas ind epresent breached and parti

to a shallower dip on this fault relative to other local faults, resulting in a lower reactivation likelihood. Of interest is the partially breached Wynn palaeocolumn. The fault associated with this trap (NE Fault 2) has been modelled to have a moderate

likelihood of dilation (~0.5 to 0.6) and slip (0.3 to 0.45, depending on fault plane roughness), which may have attributed to the partial breaching of the column due to past reactivation breaking the sealing mechanism.

Future hydrocarbon exploration within the Penola Trough area should typically be focussed initially on traps associated with E-W striking faults and towards plays between 1900 and 3800m depth, where maturity is optimal. The post-migration reactivation of many NW-SE striking fault segments has led to the increased likelihood of partial or full column breach on traps associated with such faults.

Relevance to geothermal exploration

Geothermal energy exploration contrasts hydrocarbon exploration in that it targets fault locations which currently appear to be prone to reactivation, enabling fluid flow through open fractures. Fracture networks with multiple permeable pathways will be optimum targets for geothermal testing, and as such would need to be further defined through analysis of fault rock core. Heat flow maps (Figure 17) from Jorand *et al.* (2010) show that the Penola Trough is relatively homogeneous in heat flow levels, with higher heat flow intuitively found deeper in the basin. There is a slight trend of higher heat flows seen with movement towards the south of the survey area. The trough itself is slightly warmer than the surrounding areas and ridges (Jorand *et al.* 2010). The warming trend to the south could be for various reasons, namely a thinning sediment thickness and thinner crust, or locally due to volcanic intrusions (Blevin & Cathro 2008, Petroleum and Geothermal Group 2008).

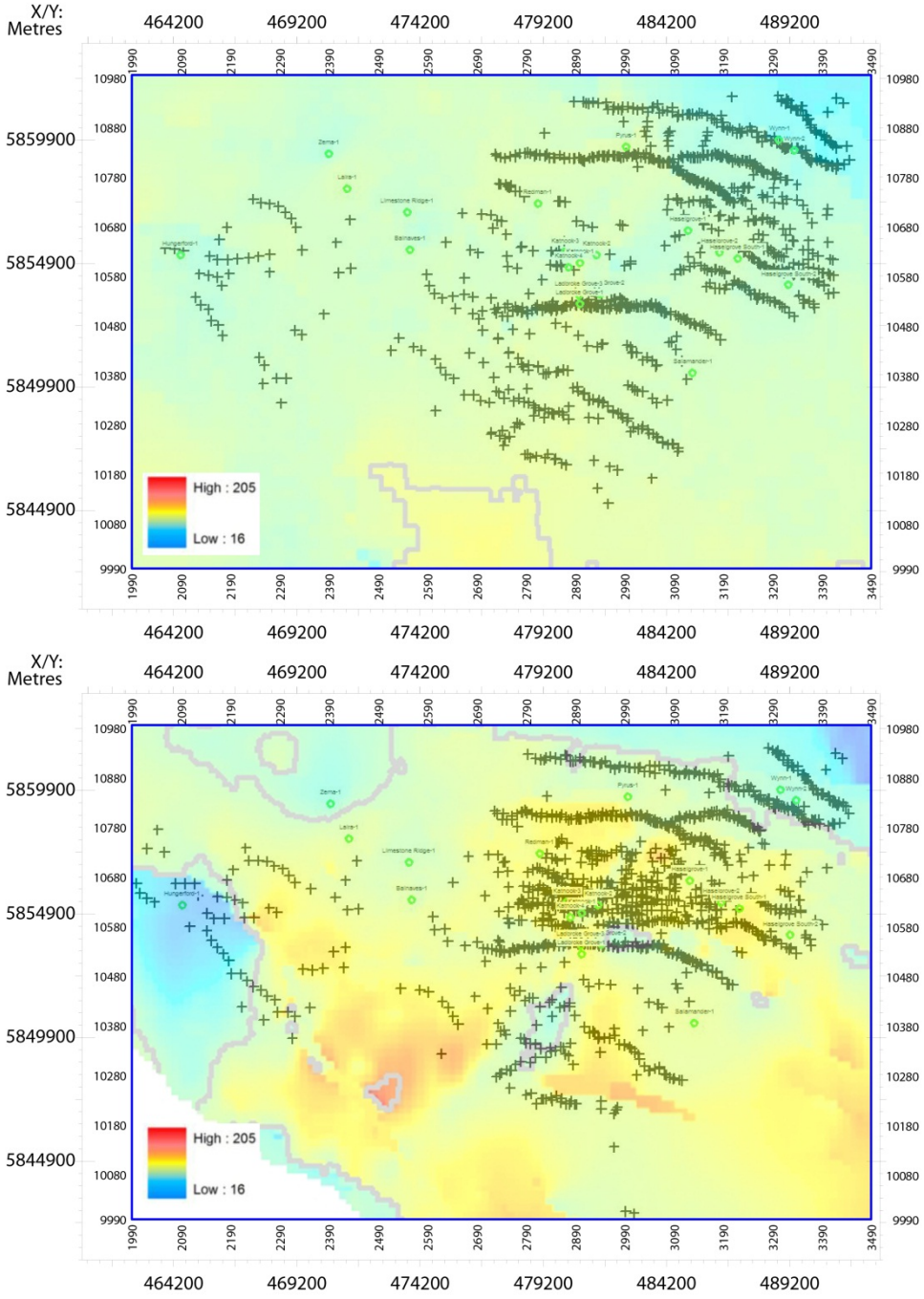

Figure 17. Horizontal slices at top Crayfish (top slice) and top Pretty Hill (bottom slice) levels showing the interpreted fault cuts (+) within the survey area, overlain with a map of heat flow (map units in degrees Celsius). Contours are at 100 degrees.

The homogeneity of heat flow leaves no location as especially preferential for geothermal targets within the survey area. As such, initial analysis of the area would lead to exploration around faults striking NW-SE, which have been shown as most likely to dilate and slip, leading to higher permeabilities. The similarities between the stress attribute models of differing lithologies lead to the conclusion that stress field characteristics play a larger part than rock properties in the reactivation likelihood of faults. Due to this, geothermal energy exploration could potentially be expanded to areas of the Otway Basin beyond the Penola Trough, so long as efforts are centred on NW-SE striking faults and their associated fracture networks. Problems may be encountered with heat flow levels, as the most likely faults to reactivate under the present stress regime are located closer to the surface, where heat flow is lesser than at depths.

Relevance to carbon dioxide sequestration

Like hydrocarbon exploration, CO_2 sequestration efforts within depleted hydrocarbon reservoirs must be centred on trap sites which have an adequate sealing mechanism. As such, CO_2 sequestration would be most successful in traps that are formed against faults that strike E-W and are positioned far from the failure envelope. Furthermore, with depth an increase in fracture stability and a decrease in likelihood of dilation and slip tendency are observed, causing the faults to theoretically become less likely to reactivate. This makes the deep Pretty Hill Sandstone an ideal target for CO_2 sequestration, as Stevens *et al*. (2001) suggest.

Supplementary information regarding reservoir rock would of course be essential before further efforts were made, however constraining possible trap geometries is an initial step. Information such as the minimum pressure following hydrocarbon depletion, as well as the maximum anticipated pressure following CO_2 injection would be necessary when calculating the stress states present in-situ. Using the stress regime knowledge, the injector well could then be located a sufficient distance away from any seismically-detectable fault planes so that local pressure highs to not influence the fault plane, causing it to become unstable via the increase in pore pressure (Hawkes *et al.* 1998).

Potential Advances

Active hydrocarbon and geothermal exploration in the Otway Basin means that new seismic surveys and borehole data are continuously being made available. The Nangwarry 3D seismic survey, to the SE of the Balnaves/Haselgrove 3D seismic survey, has already become open-file following the commencement of this project, with another well being drilled 2 years prior to the project's commencement. New exploration licenses are currently open for bids in the Penola, Robe and St. Clair troughs. Inclusion of new seismic and well control data in future similar projects would lead to a more accurate seismic interpretation of the small-scale features within the Penola Trough. The new well control would help with interpolation and extrapolation of lithology heterogeneity, as well as enabling a more accurate depth conversion to be undertaken.

Since it appears that the stress field characteristics are the most pertinent factor when modelling reactivation likelihood, constraining both stress magnitudes and orientations with higher accuracy would give a more accurate final result. The existing techniques (refer to Bell 1996, King *et al.* 2012) are able to constrain stress fields to an acceptable level. To increase the knowledge of in-situ stress fields within the Penola Trough, the number of measurements of any method must increase, providing the community with more information.

CONCLUSIONS

The results support the hypothesis that faults striking NW – SE in the Penola Trough, Otway Basin, will allow fluid flow within the in-situ stress regime. Movement of fluid requires a breach of seal, whether that is by changing the lithology juxtaposition state or cementation breakage. Dilation, fracturing and slip along faults all act to break a fault's seal. It appears that NW-SE striking fault segments are most prone to reactivation, especially at shallow depths under the current stress regime, where high end dilation and slip tendency ratios of 0.8 and up to 0.5 respectively are found. In addition to supporting this hypothesis, the results can further define the faults which may reactivate to those that are steeply dipping. This is supported by fracture stability models showing the change in pore pressures needed to cause reactivation being as little as 5 to 10MPa within the top few kilometres, compared with up to 50MPa at depth where dip is shallowest (Figure 7).

Another hypothesis in which it was presumed that a change in palaeostress regime would result in a change in reactivation likelihood was supported, with all palaeostress regimes indicating that deeper, shallowly-dipping segments, especially those striking NE-SW were more likely to have reactivated in the past, almost the opposite to present-day findings.

When coupled with hydrocarbon migration, maturity and location data, it appears that plays on E-W striking faults between 1900 and 3800 metres depth are the most likely to possess intact hydrocarbon columns. Carbon dioxide sequestration efforts are likely to be successful if focussed on traps of a similar nature or deeper. In contrast, geothermal exploration would appear to have most success in targeting the NW-SE striking fault segments which slip, dilate and fracture most easily and thus would allow water to permeate through broken fault seals and their surrounding fracture networks.

ACKNOWLEDGMENTS

Special thanks should go to the people whose knowledge and supervision enabled this project to come to fruition. Dr. Rosalind King as my primary supervisor was especially patient when assessing my work throughout the year, and all her efforts were much appreciated. Another vital thanks go to Dr. Peter Boult, Sandy Menpes and the support team at Badleys, whose knowledge of TrapTester was crucial for a trap-testing novice. Dr. Simon Holford, David Tassone, Hani Abul Khair, Ernest Swierczek and Ian West were others whose help was essential when called upon for various difficulties. Data from Andrew Krassay and the Frogtech team was also a great addition to my project. Final thanks go to the South Australian Centre for Geothermal Exploration and Research for their financial contribution to my studies.

REFERENCES

AADNOY B. S. 1990. In-situ stress direction form borehole fractures. *Journal of Petroleum Science and Engineering* **4**, 143-153.

ABUL KHAIR H., BACKÉ G., KING R., HOLFORD S., TINGAY M. R. P., COOKE D. & HAND M. 2012. Factors influencing fractures networks within Permian shale intervals in the Cooper Basin, South Australia. Australian Petroleum Production and Exploration Association 2012 Conference Exhibition, Adelaide, South Australia (unpubl.).

ANDERSON E. M. 1951. *The dynamics of faulting and dyke formation with applications to Britain* (2nd edition). Oliver and Boyd, Edinburgh.

BACKÉ G., ABUL KHAIR H., KING R. & HOLFORD S. 2011. Fracture mapping and modelling in shale gas target in the Cooper Basin, South Australia. *Australian Petroleum Production and Exploration Association* **51**, 397-410.

BADLEYS 2012. *TrapTester*. Badley Geoscience Limited, Spilsby.

BARBIER E. 2002. Geothermal energy technology and current status: an overview. *Renewable and Sustainable Energy Reviews* **6**, 3-65.

BELL J. S. 1996. Petro Geoscience 2. In situ stresses in sedimentary rocks .2. Applications of stress measurements. *Geoscience Canada* **23**, 135-153.

BELL J. S. 2003. Practical methods for estimating in situ stresses for borehole stability applications in sedimentary basins. *Journal of Petroleum Science and Engineering* **38**, 111-119.

BLEVIN J. & CATHRO D. 2008. Australian Southern Margin Synthesis. *Project GA707, Client report to Geoscience Australia by FrOGTech Pty Ltd.*

BOULT P. 2001. *Jacaranda Ridge 1, Onshore Otway Basin South Australia*. *FMS interpretation report*. Origin Energy Resources Ltd.

BOULT P., CAMAC B. & DAVIDS A. W. 2002. 3D Fault modelling and assessment of top seal structural permeability - Penola Trough, Onshore Otway Basin. *Australian Petroleum Production and Exploration Association* **42**, 151-166.

BOULT P. & HIBBURT J. E. 2002. The petroleum geology of South Australia. Volume 1: Otway Basin (2nd edition).

BOULT P., LYON P., CAMAC B., EDWARDS D. & MCKIRDY D. M. 2004. Subsurface plumbing of the Crayfish Group in the Penola Trough: Otway Basin. *Petroleum Exploration Society of Australia Eastern Australian Basins Symposium II*, pp. 483-498. Petroleum Exploration Society of Australia.

BOULT P., LYON P., CAMAC B., HUNT S. & ZWINGMANN H. 2008. Unravelling the complex structural history of the Penola Trough–revealing the St. George Fault. *Petroleum Exploration Society of Australia Eastern Australian Basin Symposium III,* Sydney, pp. 81-94.

BRUDY M. & ZOBACK M. D. 1999. Drilling-induced tensile wall-fractures: Implications for determination of in-situ stress orientations and magnitude. *International Journal of Rock Mechanics and Mining Sciences* **36**, 191-215.

CAMAC B. & HUNT S. 2009. Predicting the regional distribution of fracture networks using the distinct element numerical method. *American Association of Petroleum Geologists Bulletin* **93**, 1571-1583.

COCKSHELL C., O'BRIEN G. W., MCGEE A., LOVIBOND R., PERINCEK D. & HIGGINS R. 1995. Western Otway Crayfish Group troughs. *Australian Petroleum Production and Exploration Association* **35**, 385-404.

COSGROVE J. W. 1998. *The role of structural geology in reservoir characterisation* (Structural geology in reservoir characterisation: Geological Society Special Publication, Vol. 127).

DEWHURST D. N. & JONES R. M. 2002. Geomechanical, microstructural, and petrophysical evolution in experimentally reactivated cataclasites: Applications to fault seal prediction. *American Association of Petroleum Geologists Bulletin* **86**, 1383-1405.

DEWHURST D. N., JONES R. M., HILLIS R. R. & MILDREN S. D. 2002. Microstructural and geomechanical characterisation of fault rocks from the Carnarvon and Otway basins. *Australian Petroleum Production and Exploration Association* **42**, 167-186.

DICKINSON G. 1953. Geological aspects of abnormal reservoir pressures in Gulf Coast Louisiana. *American Association of Petroleum Geologists Bulletin* **37**, 410-432.

DUDDY I. R., EROUT B., GREEN P. F., CROWHURST P. V. & BOULT P. 2003. Timing constraints on the structural history of the western Otway Basin and implications for hydrocarbon prospectivity around the Morum High, South Australia. *Australian Petroleum Production and Exploration Association*, 59-83.

ENGELDER T. 1993. *Stress Regimes in the Lithosphere* (1st edition). Princeton University Press, Princeton.

FINLAYSON D. M., JOHNSTONE D. W., OWEN A. J. & WAKE-DYSER K. D. 1996. Deep seismic images and the tectonic framework of early rifting in the Otway Basin, Australian southern margin. *Tectonophysics* **264**, 137-152.

FISHER Q. J. & KNIPE R. J. 1998. Fault sealing processes in siliciclastic sediments. *Geological Society, London, Special Publications* **147**, 117-134.

GLUYAS J. & SWARBRICK R. 2004. *Petroleum Geoscience*. Blackwell Science Ltd.

HAWKES C. D., MCLELLAN P. J. & BACHU S. 1998. Geomechanical Factors Affecting Geological Storage of CO2 in Depleted Oil and Gas Reservoirs. *The Journal of Canadian Petroleum Technology* **44**, 52-61.

HEALY D., JONES R. R. & HOLDSWORTH R. E. 2006. New insights into the development of brittle shear fractures from a 3-D numerical model of microcrack interaction. *Earth and Planetary Science Letters* **249**, 14-28.

HILL A. J. & BOULT P. 2002a. Maturity Modelling, hydrocarbon occurence and show. *PIRSA Otway Report*.

HILL A. J. & BOULT P. 2002b. Source Rock Distribution. *PIRSA Otway Report*.

HILLIS R. R., MEYER J. J. & REYNOLDS S. D. 1998. The Australian stress map. *Exploration Geophysics* **29**, 420-427.

HILLIS R. R., MONTE S. A., TAN C. P. & WILLOUGHBY D. R. 1995. The contemporary stress field of the Otway Basin, South Australia: implications for hydrocarbon

exploration and production. *Australian Petroleum Production and Exploration Association* **35**, 494-506.

HILLIS R. R. & REYNOLDS S. D. 2002. In situ stress field of Australia. *Geological Society of Australia Special Publication* **22**, 43-52.

HOLDGATE G. R., MACKAY G. H. & SMITH G. C. 1986. The Portland Trough, Otway Basin — geology and petroleum potential. *Petroleum Exploration Society of Australia*, 292-303.

HOLDGATE G. R., RODRIGUEZ C., JOHNSTONE E. M. & WALLACE M. W. 2003. The Gippsland Basin Top Latrobe Unconformity, and its expression in other SE Australian basins. *Australian Petroleum Production and Exploration Association* **43**, 149-173.

HOLFORD S., TURNER J. P., GREEN P. F. & HILLIS R. R. 2009. Signature of cryptic sedimentary basin inversion revealed by shale compaction data in the Irish Sea, western British Isles. *Tectonics* **28**, 1-22.

HOLFORD S. P., HILLIS R. R., DUDDY I. R., GREEN P. F., STOKER M. S., TUITT A. K., BACKÉ G., TASSONE D. R. & MACDONALD J. D. 2011. Cenozoic post-breakup compressional deformation and exhumation of the Southern Australian margin. *Australian Petroleum Production and Exploration Association* **51**, 613-638.

JENSEN-SCHMIDT B., COCKSHELL C. & BOULT P. 2001. Structural and tectonic setting. *Petroleum Geology of South Australia* **1**, 1-13.

JONES R. M., BOULT P., HILLIS R. R., MILDREN S. D. & KALDI J. 2000. Integrated hydrocarbon seal evaluation in the Penola Trough, Otway Basin. *Australian Petroleum Production and Exploration Association* **40**, 263-279.

JORAND C., KRASSAY A. A. & HALL L. 2010. Otway Basin Hot Sedimentary Aquifers & SEEBASE™ Project. *Confidential Report to PIRSA-GA-DPI Vic.*

KEAREY P. & BROOKS M. 1991. *An Introduction to Geophysical Exploration* (Geoscience Texts). Blackwell Science Pty Ltd, Carlton.

KING R., HOLFORD S., HILLIS R. R., TUITT A., SWIERCZEK E., BACKÉ G., TASSONE D. R. & TINGAY M. R. P. 2012. Reassessing the in-situ stress regimes of Australia's petroleum basins. *Australian Petroleum Production and Exploration Association* **52**, 415-426.

KOPSEN E. & SCHOLEFIELD T. 1990. Prospectivity of the Otway Supergroup in the central and western Otway Basin. *Australian Petroleum Production and Exploration Association* **30**, 263-279.

KRASSAY A. A., CATHRO D. & RYAN D. J. 2004. A regional tectonostratigraphic framework for the Otway Basin. *Petroleum Exploration Society of Australia*, 97-106.

LISLE R. J. & SRIVASTAVA D. C. 2004. Test of the frictional reactivation theory for faults and validity of fault-slip analysis. *Geology* **32**, 569-572.

LOVIBOND R., SUTILL R. J., SKINNER J. E. & ABURAS A. N. 1995. The Hydrocarbon Potential of the Penola Trough, Otway Basin. *Australian Petroleum Production and Exploration Association* **35**, 358-371.

LYON P., BOULT P., HILLIS R. R. & MILDREN S. D. (Editors) 2005a. *Sealing by Shale Gouge and Subsequent Seal Breach by Reactivation: A Case Study of the Zema*

Prospect, Otway Basin. (Evaluating fault and cap rock seals: American Association of Petroleum Geologists Hedberg Series).

LYON P., BOULT P., MITCHELL A. & HILLIS R. R. 2004. Improving fault geometry interpretation through 'pseudo-depth' conversion of seismic data in the Penola Trough, Otway Basin. *Eastern Australian Basins Symposium II,* Adelaide, pp. 695-706. The Petroleum Exploration Society of Australia, Special Publication.

LYON P., BOULT P., WATSON M. & HILLIS R. R. 2005b. A systematic fault seal evaluation of the Ladbroke Grove and Pyrus traps of the Penola Trough, Otway Basin. *Australian Petroleum Production and Exploration Association* **45**, 459-476.

LYON P. J., BOULT P. J., HILLS R. R. & BIERBRAUR K. 2007. Basement controls on fault development in the Penola Trough, Otway Basin, and implications for fault-bounded hydrocarbon traps. *Australian Journal of Earth Sciences* **54**, 675-689.

MCGOWRAN B., HOLDGATE G. R., LI Q. & GALLAGHER S. J. 2004. Cenozoic stratigraphic succession in southeastern Australia. *Australian Journal of Earth Sciences* **51**, 459-496.

MULLER R. D., DYKSTERHUIS S. & REY P. 2012. Australian paleo-stress fields and tectonic reactivation over the past 100 Ma. *Australian Journal of Earth Sciences* **59**, 13-28.

NELSON E., HILLIS R. R., REYNOLDS S. D. & MILDREN S. D. 2006. Present-day state-of-stress of southeast Australia. *Australian Petroleum Production and Exploration Association* **46**, 283-305.

NORVICK M. S. & SMITH M. A. 2001. Mapping the plate tectonic reconstruction of southern and southeastern Australia and implications for petroleum systems. *Australian Petroleum Production and Exploration Association* **41**, 15-35.

PALMOWSKI D., HILL D. & HOFFMAN N. (Editors) 2004. *Structural-stratigraphic styles and evolution of the offshore Otway Basin - A structural seismic analysis*. (Eastern Australian Basins Symposium II). The Petroleum Exploration Society of Australia, Special Publication.

PERINCEK D. & COCKSHELL C. 1995. The Otway Basin: Early Cretaceous rifting to Neogene inversion. *Australian Petroleum Production and Exploration Association* **35**, 451-465.

PERINCEK D., SIMONS B. & PETTIFER G. 1994. The tectonic frame-work and associated play types of the western Otway Basin, Victoria, Australia. *Australian Petroleum Production and Exploration Association* **34**, 460-477.

PETROLEUM AND GEOTHERMAL GROUP 2008. Petroleum and Geothermal in South Australia. *The Department of Primary Industries and Resources of South Australia Petroleum Exploration Data Package*.

REYNOLDS S. D., COBLENTZ D. D. & HILLIS R. R. 2002. Tectonic forces controlling the regional intraplate stress field in continental Australia: results from new finite-element modelling. *Journal of Geophysical Research* **107**, 2131-2145.

REYNOLDS S. D. & HILLIS R. R. 2000. The in situ stress field of the Perth Basin, Australia. *Geophysical Research Letters* **27**, 3421-3424.

SANDIFORD M. 2002. Neotectonics of southeastern Australia: linking the Quaternary faulting record with siesmicity and in situ stress. *Geological Society of Australia Special Publication* **22**, 113.

STEVENS S. H., PEARCE J. M. & RIGG A. A. J. 2001. Natural Analogs for Geologic Storage of CO2: An Integrated Global Research Program. First National Conference on Carbon Sequestration, Washington, D.C. (unpubl.).

TEASDALE J., PRYER L., STUART-SMITH P., ROMMINE K., LOUTIT T., ETHERIDGE M., SHI Z., FOSS C., VIZY J., HENLEY P. & KYAN D. 2002. Otway and Sorell Basins. *SRK Consulting SEEBASE Project*.

TINGAY M. R. P., BENTHAM P., DE FEYTER A. & KELLNER A. 2011. Present-day stress-field rotations associated with evaporites in the offshore Nile Delta. *Geological Society of America Bulletin* **123**, 1171-1180.

TINGAY M. R. P., HILLIS R. R., MORLEY C. K., SWARBRICK R. & OKPERE E. C. 2003. Variation in vertical stress in the Baram Basin, Brunei: tectonic and geomechanical implications. *Marine and Petroleum Geology* **20**, 201-212.

TUITT A. K., HOLFORD S. P., HILLIS R. R., UNDERHILL J. R., RITCHIE J. D., JOHNSON H., HITCHEN K., STOKER M. S. & TASSONE D. R. 2011. Continental margin compression: A comparison between compression in the Otway Basin of the Southern Australian margin and the Rockall-Faroe area in the Northern Atlantic margin. *Australian Petroleum Production and Exploration Association* **1**, 1.

TWISS R. J. & MOORES E. M. 1992. *Structural Geology*. W.H. Freeman and Company, New York.

VEEVERS J. J. 1986. Break-up of Australia and Antarctica estimated as mid-Cretaceous (955 Ma) from magnetic and seismic data at the continental margin. *Earth and Planetary Science Letters* **77**, 91-100.

VIDAL-GILBERT S., TENTHOREY E., DEWHURST D. N., ENNIS-KING J., VAN RUTH P. J. & HILLIS R. R. 2010. Geomechanical analysis of the Naylor Field, Otway Basin, Australia: Implications for CO2injection and storage. *International Journal of Greenhouse Gas Control* **4**, 827-839.

WILLIAMS G. A., TURNER J. P. & HOLFORD S. 2005. Inversion and exhumation of the St. George's Channel basin, offshore Wales, UK. *Journal of the Geological Society* **162**, 97-110.

ZOBACK M. L. 1992. First and second order patterns of stress in the lithosphere: The world stress map project. *Journal of Geophysical Research* **97**, 703-728.

APPENDIX A: EXTENDED METHODS

Gathering data

- The Haselgrove 3D seismic survey was conducted by Geco-Prakla (Australia) Pty Ltd for Sagasco Resources between 21/02/1995 and 2/04/1995. The Haselgrove 3D seismic survey had an area of 157.10km^2.
- The Balnaves 3D Seismic survey was conducted by Schlumberger Reservoir Evaluation Seismic for Origin Energy Resources Ltd between 4/04/2000 and 20/05/2000. The Balnaves 3D seismic survey had an area of 218.50km^2.
- Reprocessing of the combined Balnaves and Haselgrove 3D seismic surveys was undertaken in February 2002 by WesternGeco. Reprocessing using a F KX KY filter resulted in significant improvement from the previously used FXCNS filter.
- A thorough background and geological history literature review was undertaken prior to the commencement of the project in order to familiarize oneself with the Otway Basin and nature of its formation and history.

Importing SEG-Y

- In this study, data from within the Balnaves-Haselgrove 3D seismic survey was viewed in both two-way-time and depth corrected vertical sections to interpret and identify faults, horizons and prominent syn-rift and post-rift packages in the Penola Trough, onshore Otway Basin, South Australia.
- SMT Kingdom Seismic Interpretation Package 8.6 (32 Bit) was used to interpret the vertical seismic sections.
- The SEG-Y Seismic Data file was imported into SMT Kingdom Seismic Interpretation Package. The inline extents of the survey were set to range from 1990 to 3490, while crosslines were inputted to range from 9990 to 10986, both with an increment of 1.
- The bin spacings were 20 metres in the inline direction and 20.0803 metres in the crossline direction.
- Corner points of the Balnaves-Haselgrove 3D seismic survey were inputted in AGD 84 datum zone 54. The inputted survey coordinates in the X (inline) direction ranged from 462503.00 to 492503.00. The coordinates in the Y (crossline) direction ranged from 5842543.70 to 5862463.70. The bottom left, top left and bottom right survey coordinates were inputted into SMT Kingdom

Seismic Interpretation Package in order to define the survey's boundaries, with the package calculating the last corner point allowing the software to define the survey's location.

- Inlines were loaded with a 16 bit integer, while crosslines were loaded with a 32 bit integer.
- The sampling interval was set to 4 milliseconds (0.004 seconds), with 5 seconds of vertical data imported.
- The start time byte location was -100 milliseconds and was inputted with a 16 bit integer.
- Data was loaded in 32 bit format.

Interpreting the survey

- When viewing the vertical seismic sections, the horizontal display scale was set to display 50 traces per inch. The vertical display scale was set to display 3 inches per second. This allowed a good view of most of the entire vertical section at the one time, eliminating the need for excessive vertical scrolling.
- Interpretation was made on strong negative or positive wavelet amplitudes. Strong positive amplitudes ("peaks") were interpreted as representing a high seismic velocity-low seismic velocity boundary (e.g. sandstone on top of mudstone). Strong negative amplitudes ("troughs") were interpreted as representing a low seismic velocity-high seismic velocity boundary (e.g. mudstone on top of sandstone). Interpretation towards the periphery of the survey was given less weighting due to the reduced fold in those areas.
- Fault interpretations were made when interpreted reflectors ended abruptly and reappeared at a shorted or longer time (shallow or deeper depth) in the vertical seismic section. Faults with minimal reflector displacement were not interpreted on. Displacement of reflectors could be viewed on both vertical seismic sections and on time slices ("lineaments") at a certain time. Faults were also interpreted on zones of zero amplitude or locations where reflectors made a sudden change in dip angle, representing a location where the seismic resolution could not detect a break in reflector.

Interpreting using well data

- 18 onshore wells were located within the combined survey areas, with data from these wells used as background to constrain the in-situ stress field, rheology and lithology conditions present within the area.
- 15 onshore wells located in the proximity (~15km) of the combined survey areas were also used to further constrain conditions, with less weighting given to the data with increasing distance from the combined seismic survey perimeter.
- Well data was also imported into SMT Kingdom Package. The same coordinates used for importing the SEG-Y file were used in order to have the well locations coincide with the location of the seismic survey.
- Horizon formation tops were manually inserted into SMT Kingdom Package from data gathered from well completion reports.
- Stratigraphic logs obtained from wells within the Balnaves-Haselgrove 3D seismic survey containing formation top data were used to help select the most appropriate reflector to interpret horizons on, as strong negative and positive reflectors often occurred in close proximity to one another.
- Interpretation was primarily undertaken on parallel arbitrary seismic lines running SSW-NNE, using a line spacing increment of 20 between each arbitrary line. This direction was chosen to run perpendicular to the NW-SE and E-W striking Penola Trough and its associated faults, in order to give an interpretation angle which would give the best seismic image. Choosing an angle perpendicular to strike removed problems associated with apparent dip of faults.
- Vertical seismic lines were viewed on either 200-colour gradient Black-to-White or Red-White-Blue colour displays. All time slice maps were also viewed using the same colour displays. Black-to-White displays were used predominantly when interpreting faults, while Red-White-Blue colour displays were used predominantly when interpreting horizons.
- 5 seismic reflectors were interpreted as prominent horizons across a large vertical proportion of the survey. These specific reflectors were chosen after consultation with the literature and were interpreted to be important horizon boundaries in the Otway Basin.
- Not all horizons were interpreted. The 5 that were chosen were assumed to be the best in terms of lateral amplitude strength resulting in reliable interpretation..

Using TrapTester

- Following initial interpretation in SMT Kingdom Package, a simplified structural interpretation was performed in Badleys TrapTester v.6.057.
- The reprocessed Balnaves/Haselgrove 3D seismic survey was loaded into Badleys TrapTester using the methods described by Badleys (2012).
- Formation top data was loaded into Badleys TrapTester using the methods described by Badleys (2012) for 6 wells located within the survey (Haselgrove-1, Haselgrove South-2, Katnook-1, Katnook-4, Redman-1 and Wynn-1), which were chosen for their proximity to the interpretation as well as the fact that they possessed velocity surveys for the subsequent depth conversion.
- A depth conversion was performed using the aforementioned velocity surveys, using the methods described by Badleys (2012).
- Structural seismic interpretation was undertaken on a series of 127 arbitrary lines, striking roughly NE-SW so as to cut perpendicular to the main structures identified in the initial SMT Kingdom Package interpretation.
- 5 faults were identified from the previous interpretation as faults that were consistently identifiable throughout the entire survey. These faults were interpreted in the depth domain in Badleys TrapTester on arbitrary vertical seismic sections.
- 3 horizons were interpreted, using the previously loaded formation tops as a rough guide for interpretation. The horizons chosen (Pebble Point Formation, Laira Formation and Pretty Hill Formation) were traceable across much of the survey, and were relevant to the subsequent analysis.
- The fault and horizon segments were modelled into surfaces.
- 7 different stress profiles were constructed (Unfaulted cataclasite, unfaulted reservoir rock, resheared cataclasite, resheared reservoir rock, 11-6Ma resheared reservoir, 23-11Ma unfaulted reservoir and 55Ma unfaulted reservoir). Each stress profile involved maximum, minimum and vertical stress magnitudes, in-situ stress orientations, pore pressures, rock coefficients of friction and rock cohesive strengths. Data for the stress profiles were gathered from various published sources (Jones *et al.* 2000, Dewhurst & Jones 2002, Dewhurst *et al.* 2002, Lyon *et al.* 2005b, Muller *et al.* 2012).
- The minimum horizontal stress used was determined from six leak-off tests and two high quality extended leak off tests.
- The maximum horizontal stress was determined by the occurrence of D.I.T.F.s in two wells using the methods described by Brudy and Zoback (1999)

- The vertical stress was calculated for five wells by integration of the density log using the methods described by Tingay *et al.* (2003)
- The maximum horizontal stress orientation was constrained from 373 borehole breakouts of A-C quality (Zoback 1992).
- The pore pressure gradient was determined from high quality formation tests and drill stem tests.
- The failure envelope, including friction coefficients and rock strengths, was determined from tri-axial testing of core samples from the Banyula-1 well, located along structure and deemed to be analogous to the survey area (Dewhurst & Jones 2002, Dewhurst *et al.* 2002).
- Relative palaeostress *regimes* (not magnitudes) from Muller *et al.*'s (2012) Gippsland Basin calculations were coupled with arbitrary palaeostress magnitudes on the same scale as present day magnitudes (11-6Ma, $\sigma_h = 20$, $\sigma_H = 25$, $\sigma_v = 15$; 23-11Ma, $\sigma_h = 20$, $\sigma_H = 25$, $\sigma_v = 15$; 55Ma, $\sigma_h = 20$, $\sigma_H = 25$, $\sigma_v = 15$)
- The 7 different stress profiles were applied to the fault surfaces, and the relevant display techniques used to show different stress attributes (dilation tendency, fracture stability and slip tendency).
- Geomechanical plots of stresses with depth, Mohr circle diagrams and stereogram projections of poles to fault planes were collected and analysed.